Klaus Witrisal, Geert Leus, Gerard J.M. Janssen, Marco Pausini,
Florian Troesch, Thomas Zasowski, and Jac Romme

Noncoherent Ultra-Wideband Systems

An overview of recent research activities

The need for low-complexity devices with low-power consumption motivates the application of suboptimal noncoherent ultra-wideband (UWB) receivers. This article provides an overview of the state of the art of recent research activities in this field. It introduces energy detection and autocorrelation receiver front ends with a focus on architectures that perform the initial signal processing tasks in the analog domain, such that the receiver does not need to sample the UWB received signals at Nyquist rate. Common signaling and multiple access schemes are reviewed for both front ends. An elaborate section illustrates various performance tradeoffs to highlight preferred system choices. Practical issues are discussed, including, for low-data-rate schemes, the allowed power allocation per pulse according to the regulator's ruling and the estimated power consumption of a receiver chip. A large part is devoted to signal processing steps needed in a digital receiver. It starts with synchronization and time-of-arrival estimation schemes, introduces studies about the narrowband interference problem, and describes solutions for high-data-rate and multiple access communications. Drastic advantages concerning complexity and robustness justify the application of noncoherent UWB systems, particularly for low-data-rate systems.

Digital Object Identifier 10.1109/MSP.2009.932617

INTRODUCTION

The wealth of advantages derived from a large signaling bandwidth has motivated considerable interest shown in the past towards UWB communication systems [1], [2]. The possibility of extremely high data rates as well as high-accuracy ranging together with the promise of low-power and low-complexity devices are some of the many features making UWB so attractive. However, UWB system design poses a number of new technical challenges, and traditional design guidelines are insufficient, or even misleading. Whereas low-complexity UWB transmitters are very feasible, especially when considering the principle of impulse radio (IR) signaling [3], there is a number

1053-5888/09/$25.00©2009IEEE

of processing tasks that, as a consequence of the large signal bandwidth, makes the implementation of conventional optimum receivers extremely complex, if feasible at all.

First of all, a fully digital receiver must be able to sample the received signal at least at the Nyquist rate, which is twice the signal bandwidth. Analog-to-digital converters (ADCs) working at such a high rate are in general very expensive and power demanding. Next, the crucial task of synchronization, which must be accomplished at the scale of subnanosecond duration, is foreseen to be extremely complex, requiring sophisticated signal processing algorithms and low clock jitter. Even more challenging is the energy capture of the multipath channel. Indeed, the very large bandwidth of the UWB signal allows for a very fine time resolution, which results in a very large number of resolvable multipath components [4], [5]. If fully exploited, the rich multipath diversity can be used to considerably reduce the fading margin, making UWB systems virtually immune to fading. However, to capture a sufficient amount of energy using a Rake receiver, a large number of correlators must be implemented, resulting in a very complex hardware architecture. Such receivers are further burdened with the problem of estimating the amplitude and the delay of each multipath component, which must be accomplished in general at a relatively low signal-to-noise ratio (SNR).

Due to these problems, there is an impellent need for simpler receiver structures, capable to exploit the rich UWB multipath channel diversity at an affordable cost, reasonable power consumption, and low complexity. Today, there is general agreement that optimum receiver structures derived for conventional narrowband communications are not feasible for low-power UWB communications, and slowly a considerable part of the research has been shifted towards the design of suboptimum, noncoherent schemes, with receiver architectures based on energy detectors (EDs) and autocorrelation receivers (AcRs). Many novel solutions and significant advances are scattered over a relatively large amount of literature.

DEFINITION OF NONCOHERENT RECEIVERS

A coherent receiver can exploit the absolute phase information of the received carrier-modulated signal, while a noncoherent energy detection receiver can only exploit the envelope, i.e., instantaneous power, of the signal. The noncoherent receiver has a complexity advantage in the sense that no coherent carrier recovery is needed.

In UWB IR, the channel impulse response of the received signal can be resolved with an extremely high time resolution due to the large signal bandwidth used, revealing up to hundreds of multipath components (MPCs) [4], [5]. In this case, the signal phase changes from MPC to MPC, as illustrated in Figure 1. A noncoherent receiver can (at best)observe the envelope of the channel response. In fact, a noncoherent UWB receiver might simply employ a squaring device and an energy integrator, as shown in Figure 2(a), such that the energy of all multipath components is accumulated within its analog front end. This architecture is called the ED. Figure 1 shows the integration window that would be chosen. A coherent receiver has to recover the phase, amplitude, and timing information of each resolvable multipath component to achieve the energy acquisition. To illustrate the involved complexity, Figure 1 depicts a set of in-phase/quadrature-phase (I/Q) sample pairs that represents a sampled version of the received pulse. The complexity advantage of the ED is apparent, although the signal bandwidth has been chosen at "only" 500 MHz in the figure, for clarity. Furthermore, phase variations have to be tracked accurately in the coherent approach, which is a big issue in practical implementations.

In narrowband as well as UWB systems, the choice of a noncoherent architecture has an impact on the modulation schemes that can be used. In case of the ED, any information on the symbol phase is lost, therefore phase-shift keying (PSK) is useless. Typically, on-off keying (OOK) and pulse-position modulation (PPM) are used, or frequency-shift keying (FSK). The latter requires a receiver with parallel bandpass filters centered at the modulation frequencies, each followed by an ED channel. The section "Signaling Schemes and Receiver Architectures" introduces typical signaling schemes used in noncoherent UWB systems.

The generic optimum noncoherent receiver is known to consist of a bank of filters matched to the transmitted candidate waveforms, followed by EDs [6]. This suggests for the UWB case that the optimum noncoherent receiver requires a filter matched to the UWB channel response prior to the ED. Clearly, this would destroy the complexity advantage, hence tradeoffs between complexity and performance have to be found. This problem has become a popular research topic that will also receive considerable attention in this tutorial (see the sections "Performance Enhancement" and "Equalization and High-Rate Noncoherent UWB").

Differential receivers exploit signal phase information by introducing a system block that performs a phase

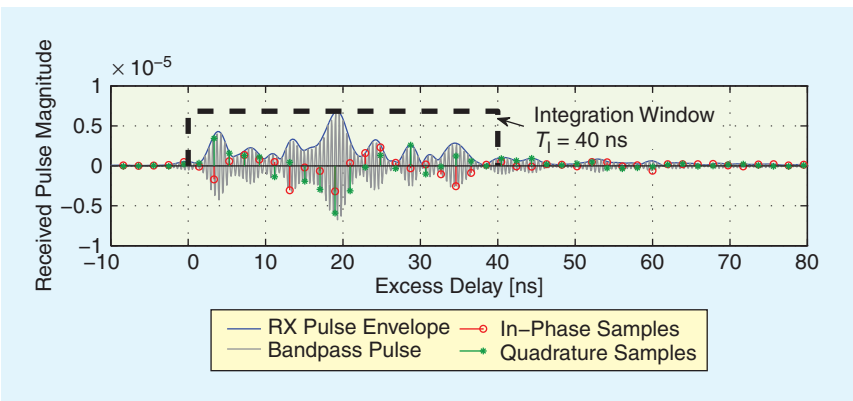

[FIG1] Received UWB pulse in a non-line-of-sight environment. The pulse bandwidth is 500 MHz, shown at a 2-GHz carrier to illustrate the phase and amplitude variations.

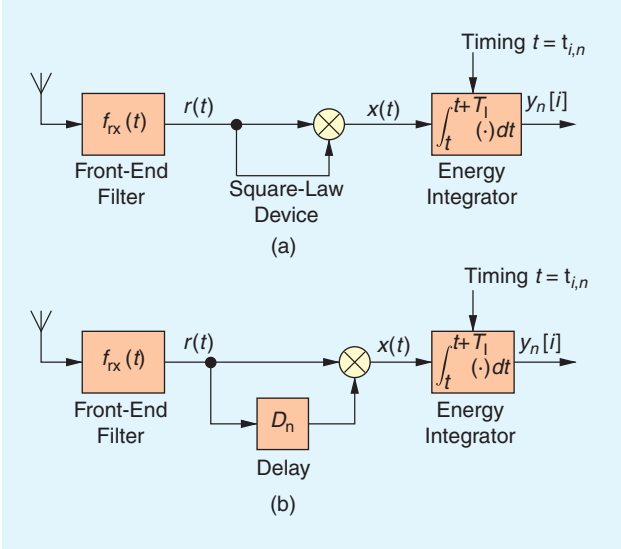

[FIG2] Receiver architectures: (a) ED and (b) AcR.

comparison between signal components. Still, no recovery of the absolute carrier phase is needed, hence we include differential detectors in the class of noncoherent receivers which are the scope of this work. In narrowband systems, the phase comparison is typically performed in the baseband after downconverting the communications signal [6]. This allows coherent accumulation of the symbol energy by a baseband filter prior to the phase comparison and is thus called differentially coherent detection.

In the UWB case, a simple receiver architecture is obtained if the phase comparison is performed prior to the energy integration. Typically, such receivers incorporate an analog delay line and a mixer to compare the signal phase at two time instants corresponding to the delay lag; see Figure 2(b). Then the output signal is accumulated, collecting the energy contained in all multipath components. This receiver concept is usually called an AcR, as its signal processing is equivalent to an analog implementation of an autocorrelation device for a fixed delay lag [7]. In UWB it is often used in conjunction with transmitted-reference (TR) signaling, where polarity [i.e., binary PSK (BPSK)] modulation of consecutive pulses carries the data information [8]–[10], or with differential phase modulation (see "Signaling Schemes and Receiver Architectures").

SCOPE

The focus of this article is on IR UWB systems, which are particularly suited for noncoherent detection. It includes so-called baseband pulse transmission schemes that do not perform carrier modulation [1] but also bandpass schemes. The latter are currently finding first applications within the IEEE 802.15.4a standard [11], which describes an alternative UWB physical layer for ranging and communications in wireless personal area networks and sensor networks.

SIGNALING SCHEMES AND RECEIVER ARCHITECTURES

ENERGY DETECTOR

The ED, which can be regarded as the classical noncoherent receiver, collects the energy of the received signal over a given time and frequency window. Such a receiver consists of a front-end filter to select the desired frequency band, a square-law device to compute the instantaneous received signal power, and an energy integrator equipped with a trigger mechanism to select either one or several time windows. This basic receiver front end is illustrated in Figure 2(a). Mathematically, the output of the ED is expressed as

$$y_n[i] = \int_{t_{i,n}}^{t_{i,n}+T_I} r^2(t)dt, \tag{1}$$

where $t_{i,n}$ denotes the start time of the nth integration window of the ith transmitted symbol, assuming that multiple samples may be acquired per symbol as indicated by the index $n = 1, \ldots, N$. The duration of the integration window is written as T_I. The samples $y_n[i]$ are usually linearly combined to form a decision variable $z[i]$ for the ith data symbol. Finally, a threshold decision is taken upon $z[i]$ using the threshold γ, such that the transmitted symbol can be estimated by $\hat{s}[i] = \text{sign}(z[i] - \gamma)$.

Some key signaling concepts are illustrated in Figure 3. The basic tradeoffs of these schemes are discussed next. Considering OOK as shown in Figure 3(a), the ED collects the energy in the time window where the received pulse is expected. Referring to the figure, note that only noise will be accumulated in the symbol interval $i = 1$, where the transmitted symbol $s[1] = 0$, while signal and noise energy will be observed in interval $i = 0$, where $s[0] = 1$. Therefore, an appropriate decision threshold is required based on input noise and signal power [13].

The complexity of decision threshold computation is avoided when binary pulse position modulation (BPPM) is used to encode the symbol $s[i]$. As seen in Figure 3(b), in each symbol interval, a pulse is transmitted whose position is determined by $s[i]$. The receiver captures two samples $y_n[i]$, $n = 1, 2$, at a distance of T_{PPM} seconds and subtracts one from another to form a decision variable $z[i] = y_1[i] - y_2[i]$. The resulting signal is either positive or negative depending on $s[i]$. A zero threshold $\gamma = 0$ can be used to decide upon $s[i]$, due to the symmetry of the samples $y_1[i]$ and $y_2[i]$. Please note that this symmetry only holds under the conditions that no inter-symbol interference (ISI) occurs, that T_{PPM} is shorter than the channel coherence time, and that the noise process is stationary. The performance of different signaling schemes is compared in the section "Performance Evaluation and Comparison." Additionally, high-rate transmission schemes are discussed in the section "Equalization and High-Rate Noncoherent UWB."

Time hopping (TH) has been suggested to support multiple access communications and for spectrum smoothing [1], [9], [14], [15], where a stream of pulses is used for each transmitted symbol. The principle of multiple access with noncoherent receivers is shown in Figure 3(c). Each data symbol is expressed by

multiple pulses whose timing is hopped in steps of T_H within so-called pulse frames, according to a TH code. The receiver integrates the incoming energy applying the transmitter's hopping pattern. Any interference occurring in between the integration intervals will be suppressed. The key problem of this concept is its inefficiency concerning the signal-to-noise ratio (SNR) at the decision device, which is further highlighted in the section "Performance Evaluation and Comparison."

Figure 3(d) illustrates the signaling scheme adopted in the IEEE 802.15.4a standard [11]. Multiple closely spaced pulses (at 2 ns intervals) are concatenated to a so-called pulse burst. A random scrambling sequence, which changes from symbol to symbol, is modulated on these pulses. The entire pulse bursts are time hopped from symbol to symbol and BPPM and BPSK modulated. Various benefits are achieved with such a signaling scheme. Foremost, the modulated data can be demodulated by noncoherent as well as coherent receiver structures. Only the latter can demodulate the BPSK information, which it employs for forward error correction. The scrambling code helps with multiple access interference (MAI) suppression (with coherent receivers) and spectral smoothing. Transmission of multiple closely spaced pulses increases the transmitted signal power, keeping the pulse power fixed. At the same time, the integration interval of an energy detector is increased by only a small increment (2 ns) per additional pulse. This makes the integration interval optimization problem (see the section "Performance Comparison and Optimization") less dependent on the unknown channel, because the effective channel spread is determined by the burst length, as elaborated in [16].

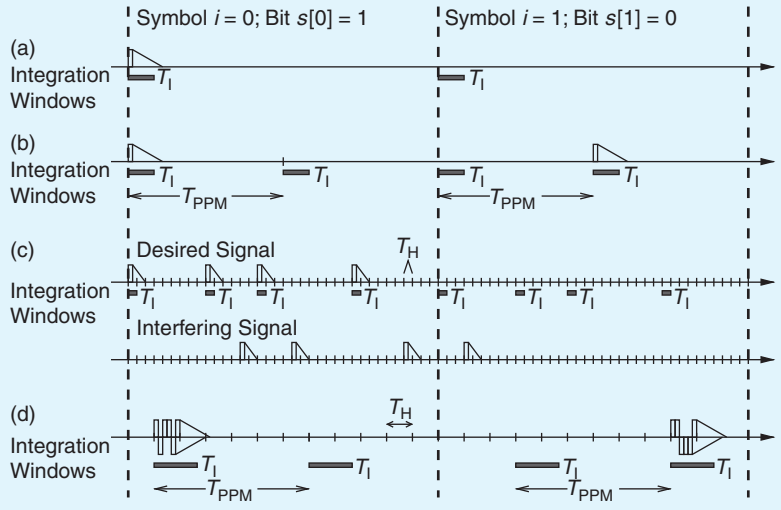

[FIG3] Signaling schemes for the energy detector: (a) OOK, (b) BPPM, (c) OOK with time hopping and an asynchronous interfering signal with different TH code, and (d) BPPM with randomly encoded pulse bursts and TH.

AUTOCORRELATION RECEIVER

The AcR replaces the square-law device of the ED by a delay element and a multiplier, as shown in Figure 2(b) [7]–[10]. The delay aligns the first of two consecutively transmitted pulses such that it can serve as a noisy template for the demodulation of the second pulse, which is PSK-modulated by the data symbol. Thereby, the AcR collects energy from all multipath components, just like the ED. In fact, the delay (of D seconds) and the multiplier lead to an instantaneous phase comparison of signal parts spaced by D seconds. The integrator accumulates the signal energy of these repeated signal components. Hence, the AcR selectively accumulates signal energy. It is tuned via the delay lag D. Note that the receiver as drawn in Figure 2(b) achieves a comparison of the signal signs only. A phase comparison is obtained if a frequency downconversion to baseband is performed prior the AcR processing. In [17] it has been shown that a phase comparison is also achieved with an AcR structure having two parallel channels at a delay offset of $1/(4f_c)$, where f_c denotes the carrier frequency. Mathematically, the output of the generic AcR is expressed as

$$y_n[i] = \int_{t_{i,n}}^{t_{i,n}+T_I} r(t)r(t + D_n)dt. \tag{2}$$

Please note that the AcR approaches the ED in case that $D \to 0$. However, multiple samples per symbol can be captured either by changing the integration time windows as with the ED, or by implementing multiple AcR channels with various delay lags $\{D_n\}$. This additional degree of freedom is reflected in the large variety of signaling schemes that have been studied for AcR receivers. Some key concepts are discussed next.

In Figure 4(a), the basic transmitted-reference (TR) signaling scheme is illustrated [7]–[9]. Pulse pairs, sometimes called doublets, are transmitted, consisting of an unmodulated reference pulse (white rectangle) and a differentially phase modulated data pulse (shaded rectangle), with a time spacing of D seconds. The differential modulation by $d[0] = -1$ in symbol interval $i = 0$ will lead to a negative sign of the accumulated symbol energy at the AcR output, while in symbol interval $i = 1$ a positive output will be observed. Therefore, a simple threshold detector can be used to demodulate the data. According to the illustrated timing scheme, interpulse interference (IPI) and ISI are avoided, which requires a relatively long pulse spacing $D > T_{max}$ (where T_{max} denotes the total delay spread of the multipath channel) and thus a long delay line that may be hard to implement. It also leads to a limited data rate $R = 1/T$, since $T \geq 2T_{max}$. The effect of admitting IPI and ISI will be discussed in the sections "Fading and Interpulse Interference" and "Equalization and High-Rate Noncoherent UWB," respectively.

Further signaling options for TR schemes are reflected in the well-known delay-hopped signaling scheme proposed by Hoctor

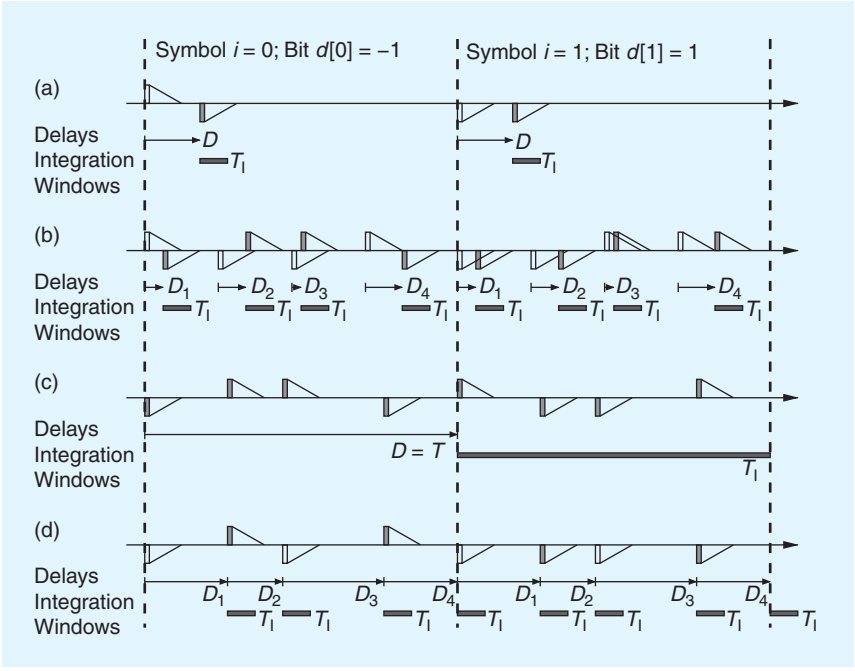

[FIG4] Signaling schemes for the autocorrelation receiver: (a) Dual-pulse TR scheme, (b) delay-hopped TR signaling, (c) symbol-differential signaling with time hopping, and (d) frame-differential signaling with delay hopping.

and Tomlinson [10]. In this scheme, which is shown in Figure 4(b), data are differentially encoded between reference and data pulses (white and shaded rectangles, respectively). However, to achieve spread-spectrum multiple access communications, the data bits are represented by a delay-hopping code, i.e., a set of pulse doublets that are spaced according to a distinct sequence of delays $\{D_n\}$. Additionally, their amplitude may be encoded with a binary sequence, which has been omitted in the figure for clarity. The receiver selects the delays of its AcRs according to the delay-hopping code and combines their outputs using the binary sequence. This way, the energy of the desired signal is selectively captured. The conceptual elegance of the scheme is hindered by the fact that again noise energy is accumulated over each integration interval, while only a fraction of the symbol energy can be assigned to each pulse doublet, similar to the time-hopped ED scheme discussed in Figure 3(c). A mitigation of this effect is achieved, if the pulses are coherently combined before the AcR processing, for instance by implementing a pre-AcR linear filter matched to the transmitted pulse sequence [18], [19]. The performance tradeoffs of different AcR realizations are elaborated in the section "Performance Evaluation and Comparison." Note that the figure indicates that IPI is admitted in this signaling scheme.

The efficiency of TR schemes is reduced because of the transmission of an explicit reference, consuming half of the symbol energy. This is avoided in so-called differential schemes, where consecutive symbols [20] [see Figure 4(c)] or consecutive frames [19], [21], [22] [see Figure 4(d)] are differentially modulated. Comparing the two options, the symbol-differential scheme would need a rather long delay line if several pulses are transmitted per bit and if long symbol periods are used to avoid ISI. However, optimal performance is achieved if only one pulse is used per symbol [21] as shown in the section "Performance Evaluation and Comparison." For this case both schemes are identical.

The big issue with TR schemes is the difficulty of integrating UWB delay lines on silicon. Analog filter structures can be used, but it seems infeasible to achieve delay values greater than a few nanoseconds [23]. Digital implementations are very power demanding. A promising alternative is the slightly frequency-shifted TR scheme proposed in [24]. In this scheme, the data waveform is made orthogonal to the reference by shifting its frequency by the symbol rate $1/T$. It is assumed that this shift is much less than the coherence bandwidth of the multipath channel, thus both signals experience equivalent distortions. The receiver employs a mixer to compensate for the frequency shift instead of the delay line in Figure 2(b). An important interpretation of this receiver follows from recognizing that the multiplication is commutative. Therefore, the mixer can be shifted behind the multiplier, which yields an ED according to Figure 2(a), where the signal $x(t)$ is multiplied by a sinusoidal at $1/T$. Just as regular ED schemes, this scheme is suitable for very limited data rates only (see the section "Equalization and High-Rate Noncoherent UWB," [24]). It can be extended to a differential multicarrier system as shown in [25], and the frequency-shifting can be replaced by code multiplexing; see [26].

PERFORMANCE EVALUATION AND COMPARISON

PERFORMANCE EVALUATION

The first goal of this section is a comparison of various receiver architectures and signaling options. For that purpose, we assume a transmission without ISI and IPI and with perfect synchronization of the integration window. In addition, we assume that the delay line in the AcR is perfectly matched to the lag between reference and data pulses, and that these two pulses undergo the same channel distortion, i.e., the multipath channel is time-invariant. Without loss of generality we assume that the received pulse of interest starts at time $t = 0$ and we drop the symbol index i and the frame index n.

With the above definitions, and using (1) and (2), we can write the sampled output of a generic receiver front end as

$$y = \int_0^{T_I} [x_0 g(t) + \nu_0(t)] \times [x_1 g(t) + \nu_1(t)] dt, \qquad (3)$$

where $x_0 = x_1 = s \in \{0, 1\}$ is the binary symbol used to express OOK and PPM with the ED, while $x_0 = 1$ and $x_1 = d \in \{\pm 1\}$ express the BPSK modulation used with TR signaling and the

AcR. The signal $g(t)$ indicates the received pulse and $\nu_0(t)$, $\nu_1(t)$ are additive Gaussian noise processes. Note that actually $\nu_0(t) = \nu_1(t)$ when an ED is employed. Expanding the product, the three well-known terms that describe the decision statistics of noncoherent UWB receivers are obtained. That is

$$\begin{aligned} y &= x_1 \int_0^{T_\mathrm{I}} g^2(t)dt + x_0 \int_0^{T_\mathrm{I}} g(t)[\nu_0(t) + \nu_1(t)]dt + \int_0^{T_\mathrm{I}} \nu_0(t)\nu_1(t)dt \\ &= x_1 h E_\mathrm{p} + x_0 \eta_l + \eta_x \end{aligned} \tag{4}$$

where we distinguish the data-modulated desired term $x_1 h E_\mathrm{p}$, a linear noise term $x_0\eta_l$, and the noise-by-noise product term η_x. The desired term expresses the instantaneous received pulse energy $\int_0^{T_\mathrm{I}} g^2(t)dt = hE_\mathrm{p}$. It has been decomposed in a channel coefficient h, which can express fading or an incomplete energy capture due to a mismatch of the integration interval with the pulse timing, and in a mean pulse energy E_p.

For a performance evaluation, we need to characterize the noise statistics. The linear noise term is Gaussian with zero mean and variance of

$$\mathrm{var}\{\eta_l\} \approx \frac{N_0}{2} \begin{cases} 2hE_\mathrm{p} & \text{AcR} \\ 4hE_\mathrm{p} & \text{ED.} \end{cases} \tag{5}$$

Hence, η_l depends on the received pulse energy just as the desired term, with fading and energy capture expressed by the same channel coefficient h. The variance doubles for the ED because $\nu_0(t) = \nu_1(t)$, while for the AcR, the two noise processes can be assumed uncorrelated. The derivation of these variances can be found for instance in [7], [27], and [28]. It assumes that the front-end filter does not influence the received signal spectrum.

The noise-by-noise product term is zero-mean if $\nu_0(t)$ and $\nu_1(t)$ are uncorrelated. If $\nu_0(t) = \nu_1(t)$, it has a mean value $\mathrm{E}\{\eta_x\} = N_0 T_\mathrm{I} W_\mathrm{rx}$, where W_rx is the equivalent noise bandwidth of the receiver front end. Its variance is

$$\mathrm{var}\{\eta_x\} \approx \frac{N_0^2}{2} \begin{cases} T_\mathrm{I} W_\mathrm{rx} & \text{AcR} \\ 2T_\mathrm{I} W_\mathrm{rx} & \text{ED,} \end{cases} \tag{6}$$

which again doubles for ED schemes, where $\nu_0(t) = \nu_1(t)$. It has been suggested that a Gaussian approximation can be used for η_x, since $\nu_0(t)\nu_1(t)$ for $t \in [0, T_\mathrm{I}]$ can be decomposed in a sum of approximately $2T_\mathrm{I}W_\mathrm{rx}$ independent random variables, hence the central limit theorem (CLT) applies for UWB systems, where $T_\mathrm{I}W_\mathrm{rx} \gg 1$ [7], [27], [28]. With this statistical characterization, the well-known Q-function can be employed to approximate the error probabilities of various transmission schemes. Exact studies of the PDF of this term can be found for instance in [18], [28], and [29]. We will next specialize the above results.

ED with BPPM

Each pulse has an energy of $E_\mathrm{p} = E_\mathrm{b}/N_\mathrm{f}$, where E_b is the energy per bit and N_f is the number of frames per symbol. The decision variable $z[i] = \sum_{n=1}^{N_\mathrm{f}} y_{2n-1}[i] - y_{2n}[i]$ is formed from differences of N_f sample pairs captured over integration intervals spaced by T_PPM (see the section "Energy Detector"). With these definitions, the noise variances of (5) and (6), and a decision threshold of zero, the instantaneous probability of error is approximated as (see, e.g., [27])

$$P_{e|h} \approx Q\left(\sqrt{\frac{1}{2}\frac{(hE_\mathrm{b}/N_0)^2}{hE_\mathrm{b}/N_0 + N_\mathrm{f}T_\mathrm{I}W_\mathrm{rx}}}\right). \tag{7}$$

The function $Q(x)$ is monotonically decreasing. This means a performance degradation when increasing the bandwidth W_rx, or the number of pulses per symbol N_f, because the noise-by-noise product term η_x is raised. The integration interval T_I also affects the collected energy hE_p, as discussed in the section "Performance Comparison and Optimization." Optimal performance is thus obtained when η_x is negligible with respect to η_l. Then the bit error rate (BER) becomes $P_{e|h}^{\mathrm{opt}} = Q(\sqrt{hE_\mathrm{b}/(2N_0)})$, which is 3 dB behind the matched filter bound for binary orthogonal signaling (with ideal coherent detection) and 6 dB behind binary antipodal signaling [30].

ED with OOK

With binary OOK, twice the energy can be assigned to actually transmitted pulses, because half the energy is saved on the "off" symbols. That is, $E_\mathrm{p} = 2E_\mathrm{b}/N_\mathrm{f}$. Furthermore, only half as much noise is accumulated, because only one integration interval is considered per pulse. With these definitions, the statistical moments of the decision variable can be obtained from the equations above. To compute the error probability, their probability density functions (PDFs) also need to be taken into account. A sampling expansion reveals that a central and a noncentral chi-squared PDF are exact statistical models for y [31]. Applying again a Gaussian approximation, which is valid for $2N_\mathrm{f}T_\mathrm{I}W_\mathrm{rx} > 40$ according to [27], and opting for a decision rule based on equal conditioned error probabilities for the two binary symbols [instead of the maximum likelihood (ML) rule], a simplified error probability formula has been derived in [27] and [31]

$$P_{e|h} \approx Q\left(\frac{2hE_\mathrm{b}/N_0}{\sqrt{N_\mathrm{f}T_\mathrm{I}W_\mathrm{rx}} + \sqrt{N_\mathrm{f}T_\mathrm{I}W_\mathrm{rx} + 4hE_\mathrm{b}/N_0}}\right). \tag{8}$$

AcR with TR Signaling

With TR signaling, the first pulse $g(t)$ in (3) is the (fixed) reference pulse, while the second pulse is differentially modulated by the data symbol d. Both pulses are normally assigned the same energy (see [32]), which thus drops to $E_\mathrm{p} = E_\mathrm{b}/(2N_\mathrm{f})$. The reduced signal energy is compensated by a reduced noise energy, as $\nu_0(t)$ and $\nu_1(t)$ are independent noise processes in this case, see (5) and (6). For this reason, it can be shown that the performance of TR signaling is equivalent to the performance of BPPM (7) [27], in absence of ISI (see [33]).

AcR with Differential Signaling

Differential signaling saves the energy used for the reference pulse in TR signaling. It thus performs exactly 3 dB better than the TR scheme. This holds for the symbol differential signaling scheme of

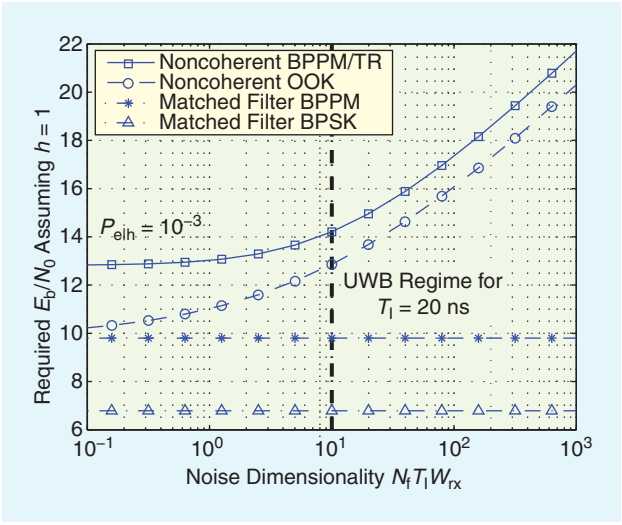

[FIG5] Performance of coherent and noncoherent UWB transceivers with normalized received pulse energy. The required E_b/N_0 to reach $P_{e|h} = 10^{-3}$ is shown.

Figure 4(c) in general, and for the frame differential scheme of Figure 4(d) if $N_f = 1$. In [19], [21], and [29], the performance has been evaluated for frame differential signaling with $N_f > 1$.

PERFORMANCE COMPARISON AND OPTIMIZATION

Noise Dimensionality

Figure 5 illustrates the required E_b/N_0 to reach a certain error probability as a function of the "noise dimensionality," which is defined as the product $N_f T_I W_{rx}$ of bandwidth, integration interval, and number of frames per symbol. It has been derived from the approximate error probabilities discussed above. The channel coefficient was normalized to $h = 1$, assuming no fading and full energy capture. As anticipated, the product $N_f T_I W_{rx}$ has to be kept as low as possible for the noncoherent receivers to minimize the required E_b/N_0. Asymptotically, doubling $N_f T_I W_{rx}$ results in an increase of 1.5 dB of required E_b/N_0. But what values are realistic for UWB systems? To be able to fully capture the energy of the received pulses, T_I has to be set longer than the channel delay spread. Assume an indoor channel with a root mean square (RMS) delay spread of about 10 ns and an approximately exponentially decaying power delay profile. Then we could set $T_I = 20$ ns to capture about 85 % of the pulse energy, as discussed below. With the minimum UWB bandwidth, defined by the Federal Communications Commission (FCC) as 500 MHz [12], this yields $N_f T_I W_{rx} \geq 10$, which is indicated in the figure as the "UWB regime."

The conclusion drawn is that it is not efficient from a performance viewpoint to increase the number of pulses per symbol. On the other hand, multiple pulses per symbol could improve the robustness against MAI or NBI, see the sections "Signaling Schemes and Receiver Architectures" and "Receiver Signal Processing." It does not seem efficient to increase the bandwidth, either. However, this does not hold if we consider the limitation of transmitted power spectral density, according to the regulator [12]. In fact 3 dB more transmit power is allowed if the bandwidth is doubled, thus the SNR loss (see also the section "Power Limit Considerations, Complexity, and Implementation Aspects") seems to be over compensated. But this only applies to a certain extent, since also the path-loss increases with frequency [16]. For the integration interval, a tradeoff exists between the energy capture and the acquired noise power, which has been investigated in numerous studies [27], [29], [32], [34], [35]. We will review the major results in the section "Integration Interval."

Comparing the various transmission schemes, it is confirmed that OOK modulation with energy detection outperforms the TR and BPPM schemes. Its advantage is 1.5 dB at large $N_f T_I W_{rx}$, and it increases to 3 dB in the non-UWB regime, where it approaches the performance of the matched-filter bound for orthogonal modulation schemes. Note that the Gaussian approximation may no longer apply if $N_f T_I W_{rx}$ is reduced. On the other hand, the noise-by-noise product term η_x is less dominant than the linear Gaussian noise term η_l where the curves flatten out. Humblet and Azizoglu [31] have analyzed that indeed the approximated error probability is still remarkably close to the exact result, in such cases. Multicarrier UWB systems are a way forward to exploit a reduced $N_f T_I W_{rx}$ product, because the bandwidth can be reduced for each subcarrier. Multicarrier schemes are discussed in the section "Equalization and High-Rate Noncoherent UWB."

The performance penalty w.r.t. coherent matched-filter receivers amounts to at least 3–4 dB for BPPM in the UWB regime, and another 3 dB for BPSK, assuming perfect channel estimation and synchronization. However, only coherent receivers can exploit the absolute phase information of BPSK. This has been used in IEEE 802.15.4a [11] and in [36] to encode redundant information for error correction coding schemes. High-complexity coherent receivers can extract this information and obtain an additional performance gain compared with noncoherent low-complexity receivers, while full compatibility of both receiver types is maintained.

Integration Interval

The benefit of integration interval (T_I) optimization has been addressed in numerous works on noncoherent UWB systems [27], [29], [32], [34], [35]. We adopt in Figure 6 the presentation of Dubouloz et al. to illustrate the performance tradeoff [27]. This has been generated by defining the energy capture as a function of T_I through the channel coefficient h. That is, we define E_b/N_0 as the receiver input SNR assuming full energy capture and we let h be the fraction of energy that is actually captured. We assume an NLOS channel with exponentially decaying power delay profile. Hence we can define $h = 1 - e^{-T_I/\tau_{rms}}$, where τ_{rms} is the RMS delay spread of the channel, and obtain the required E_b/N_0 by (7) for BPPM or TR signaling and for a fixed $N_f W_{rx}$.

The optimum is seen to depend on the desired error rate performance $P_{e|h}$ and on τ_{rms}. While the impact of $P_{e|h}$ is rather weak, the delay spread has a significant influence on the optimal T_I. A higher E_b/N_0 is needed for a longer channel, as a longer integration interval is required to capture the useful multipath energy, which implies that more noise energy is collected. It is important

to remark again that fading has been neglected in this analysis. Fading increases for reduced integration intervals due to reduced multipath diversity, causing an additional performance penalty (see the section "Fading and Interpulse Interference").

Even though rather simple mathematical models are employed, a closed-form analytic solution does not exist for this optimization problem, to the authors' best knowledge. An analysis of the asymptotic cases (where the noise-by-noise term is either dominant or negligible) reveals a simple approximation, which can be used to observe basic properties of the solution. We get (for the BPPM/TR system)

$$T_{\mathrm{I}} \approx \tau_{\mathrm{rms}} \ln\left(\frac{E_{\mathrm{b}}}{N_0}\frac{1}{N_{\mathrm{f}}W_{\mathrm{rx}}\tau_{\mathrm{rms}}} + e^{1.2564}\right), \tag{9}$$

which illustrates that the optimal integration interval is proportional to the channel's RMS delay spread, with a proportionality factor determined by E_{b}/N_0 and the product $N_{\mathrm{f}}W_{\mathrm{rx}}\tau_{\mathrm{rms}}$ (see [29 and 37]). If the product noise term η_x dominates, i.e., when $N_{\mathrm{f}}W_{\mathrm{rx}}\tau_{\mathrm{rms}}$ is much greater than E_{b}/N_0 (long channel and/or large bandwidth), then the proportionality factor converges to the constant 1.2564, the solution to $e^x = 2x + 1$. If η_x is negligible, then the factor increases linearly with the dB-value of E_{b}/N_0. This means that increasing the integration interval is beneficial as more energy is captured from the channel. As a rule of thumb, it is appropriate to set the integration interval to about one and a half to two times the τ_{rms}, where already 80–85% of the received energy (see [34]) but at most 1–2 dB of excess noise are captured.

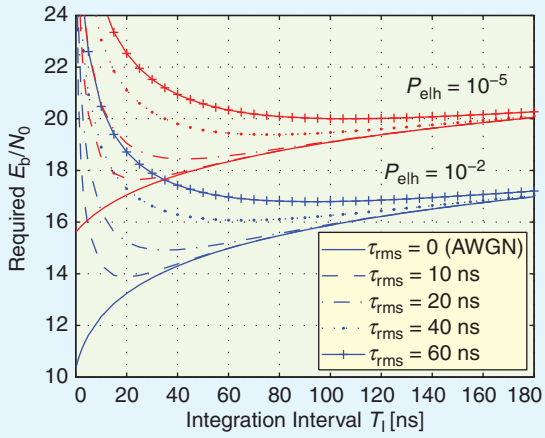

[FIG6] Optimization of the integration interval T_{I} as function of the RMS channel delay spread and the error probability. The performance is shown for BPPM/TR systems with $N_{\mathrm{f}}W_{\mathrm{rx}}$ = 1 GHz.

PERFORMANCE ENHANCEMENT

Pulse Averaging

The first method frequently considered to enhance the performance of noncoherent UWB receivers, in particular for AcR structures, is a pre-AcR pulse averaging [7], [18], [38], [39]. A coherent sum of the received signals is computed, for instance by delaying the input signals and then adding them up, before the nonlinear autocorrelation operation is performed. This approach actually corresponds to the generalized ML detector, when it is assumed that the shape of the received signal is unknown, as shown in [19]. We can incorporate the idea in the performance evaluations by defining $g(t)$ and $\nu_l(t)$, $l = 0, 1$, as sums of pulses and noise processes, respectively. Assuming that N denotes the number of averaged pulses, we introduce a scaling by $1/\sqrt{N}$ to keep the variances of the summed noise processes at their original level, and obtain

$$\bar{g}(t) = \frac{1}{\sqrt{N}}\sum_{n=1}^{N} g_n(t) = \sqrt{N}\,g(t)$$
$$\nu_l(t) = \frac{1}{\sqrt{N}}\sum_{n=1}^{N} \nu_{l,n}(t),$$

where $g_n(t)$ and $\nu_{l,n}(t)$ are the received pulses and additive noise signals after time alignment, respectively. Equivalently as before, (4)–(6) can be used to compute the statistics of the decision variable.

Let's assume that N reference pulses (taken from previous symbols) are averaged to get an enhanced template for demodulating a data symbol conveyed on a single pulse ($N_{\mathrm{f}} = 1$) [7], [38], [39]. That is, the energy of each pulse is $E_{\mathrm{b}}/2$, and we obtain $E_{\bar{g}g} = \sqrt{N}E_{\mathrm{b}}/2$, $\mathrm{var}\{\eta_l\} = N_0 h E_{\mathrm{b}}(N+1)/4$, and $\mathrm{var}\{\eta_x\} = N_0^2 T_{\mathrm{I}} W_{\mathrm{rx}}/2$, leading to

$$P_{e|h} \approx Q\left(\sqrt{\frac{1}{2}\frac{(hE_{\mathrm{b}}/N_0)^2}{\frac{1}{2}\left(1+\frac{1}{N}\right)hE_{\mathrm{b}}/N_0 + T_{\mathrm{I}}W_{\mathrm{rx}}/N}}\right). \tag{10}$$

This result is discussed in Figure 7. The equation shows that the linear noise term is reduced by a factor $1/2(1 + 1/N)$ [see (7)], which is approaching 1/2 for $N \to \infty$. This corresponds to a reduction of the required E_{b}/N_0 at low $T_{\mathrm{I}}W_{\mathrm{rx}}$ by up to 3 dB. The variance of the noise-by-noise-product term is reduced by a factor of N. This means that the point where this term becomes dominant is shifted to higher values of $T_{\mathrm{I}}W_{\mathrm{rx}}$. The gain approaches 3 dB for doubling N, at very large $T_{\mathrm{I}}W_{\mathrm{rx}}$. Asymptotically, the performance of a coherent receiver with binary orthogonal signaling is obtained, which simply corresponds to the fact that a perfect template is estimated in this case. The drawback of this technique lies in the ability to implement analog delay lines to realize such a scheme. A digital implementation is presumably needed.

The hybrid matched filter receiver of [18] coherently combines the reference as well as the data pulses. However, only pulses of one symbol are used in the detection. Therefore this receiver cannot outperform a conventional TR scheme with one pulse per frame. But it does not suffer from an increased noise dimensionality when $N_{\mathrm{f}} > 1$ pulses are used per symbol. So it is potentially of greater robustness against MAI and NBI without performance penalty. The pre-AcR combining is a step towards an optimal pre-filtering of the received signal, as performed in differentially coherent detection of narrowband signals (see the section "Definition of Noncoherent Receivers"). In fact, the optimal prefiltering, using a filter matched to the received pulse, would lead to a noise dimensionality of one.

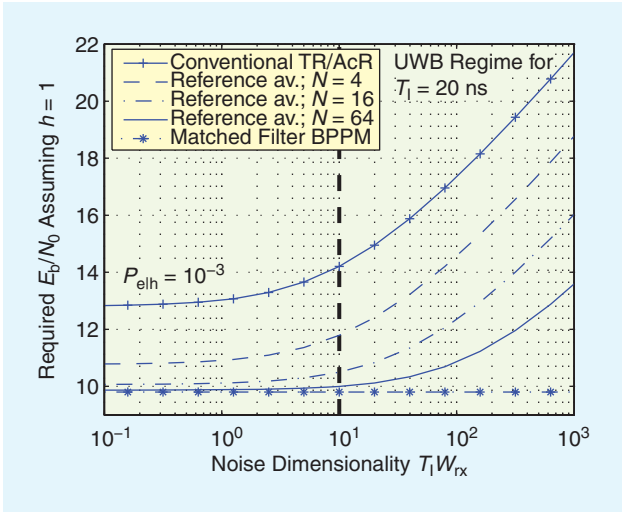

[FIG7] Performance gain obtained with reference pulse averaging as a function of the noise-dimensionality $T_l W_{rx}$.

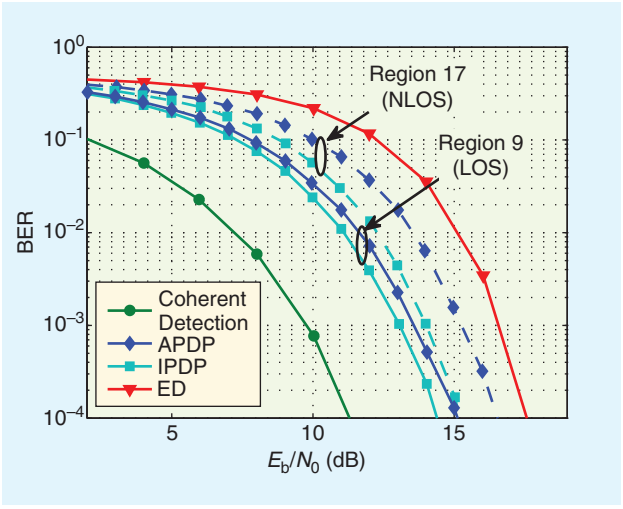

[FIG8] Performance of BPPM schemes with weighted noncoherent detection, assuming knowledge of different levels of channel state information [49].

Weighted Noncoherent Receivers

Another concept proposed for enhancing noncoherent UWB receivers are linear weighting schemes, which multiply some weighting function on the output signal $x(t)$ of the squaring device or multiplier before integrating the energy of the received pulses (see Figure 2). This way, the receiver can suppress noise in portions of the channel impulse response that don't convey (much) energy, while emphasizing strong components.

Two variants have been studied. One simply assumes that more than one sample is acquired per received symbol, i.e., the integration interval illustrated in Figure 1 is divided in a number of subintervals. It thus produces a fractionally sampled output stream of the received signal energy, which is then optimized by digital signal processing in the back-end [40]–[43]. All papers show performance improvements in the order of 1–3 dB. The influence of the number of samples taken and estimation of the required channel state information are studied in [40]. In [41], there is a focus on blind signal processing algorithms that perform the linear combining, while reference [42] demonstrates and explains that even ISI can be reduced with such a receiver front end (see the section "Equalization and High-Rate Noncoherent UWB"). Most papers also note that implicitly, this principle takes care of a synchronization for the phase of the symbol clock (see the section "Synchronization and Time-of-Arrival Estimation").

The second variant tries to approach the limits of this scheme, by allowing for weighting functions with a bandwidth up to the Nyquist frequency. That is, it is assumed that the weighting after the noncoherent receiver processing can be performed with an arbitrarily large number of samples. Weisenhorn [44] derives the maximum-likelihood receiver for BPPM signaling, assuming that the receiver has prior knowledge of the power delay profile of the channel, and finds that a weighted ED receiver is obtained. Similar work has been presented in [32] and [45] for TR receivers. Variants of this technique employ an instantaneous power delay profile (IPDP) or an average power delay profile (APDP) of the channel, which requires the availability of different levels of channel state information [46]. It has been shown that this principle can also enhance the robustness against ISI [46] and NBI [47] (see the section "Receiver Signal Processing"). Also note, if no channel state information is available, the ED is in fact the generalized ML detector for PPM signals, see [46] and [46].

It is more difficult to obtain generic performance results for this technique. The derivation in [44] allows for an insightful interpretation of the optimal weighting function that also allows conclusions on the achievable gains. When the linear noise contribution dominates, the weighting function is simply a constant. That is, no weighting is needed and no gain can be obtained. On the other hand, the weighting function is proportional to the square of the APDP, when the product noise term dominates. In this case, more gain is possible. Even better results are achieved when the IPDP can be taken into consideration, as shown in Figure 8 [49]. Note that the line-of-sight (LOS) scenario permits a higher gain than the non-LOS (NLOS) scenario, due to a powerful direct path.

FADING AND INTERPULSE INTERFERENCE

The analysis and characterization of fading is of fundamental importance to the design of mobile communications systems. To some extent, however, this is relaxed for UWB systems because the frequency diversity of the fading channel can be well exploited due to the very large bandwidth. Still some fading may remain, because individual multipath components will interfere in the channel impulse responses [50].

The channel coefficient h has been introduced in (4) to express the fading of the received pulse energy for individual channel realizations. To compute the average BER for an ensemble of channels, the error probability from (7) or (8) has to be averaged over the random variable h. This yields

$$\overline{P_e} = \int_0^\infty P_{e|h}(\xi) f_h(\xi) d\xi,$$

where $f_h(\xi)$ is the PDF of h.

It is a challenging problem to derive the PDF of h and perform the averaging [28], [51]. To solve this problem, a theoretical framework has been developed in [28] based on a sampling expansion. Exact and approximate distributions have been derived for $f_h(\xi)$ in [51]. A rougher approximation has been proposed in [52], where a log-normal PDF is used for $f_h(\xi)$. The advantage of the latter approach is that it relates the mean and variance of the log-normal PDF directly to parameters of the radio channel and UWB system—parameters like the RMS delay spread, bandwidth, and integration interval. The performance results shown in Figure 9, which compare several TR schemes, have been derived by this method. A channel with an RMS delay spread of 10 ns, an integration interval of 20 ns, and two different signal bandwidths have been considered. The solid lines show the receiver performance if interference between the reference and data pulses (IPI) is avoided. Clearly, the receiver at 5 GHz suffers from enhanced noise, as discussed in the section "Performance Comparison and Optimization." On the other hand, its performance curve is steeper due to the increased bandwidth, which shows that it can exploit multipath (= frequency) diversity much better.

Assume next that interference is admitted between the received pulses (IPI), for instance, to use an AcR with a delay line much shorter than the channel delay spread. In [50], a theoretical framework has been developed that allows a statistical evaluation of IPI. The results have been employed in [52] to include the effects of IPI in the parameters of the log-normal PDF used for $f_h(\xi)$. Hence the impact of IPI can be evaluated analytically. Figure 9 illustrates the resulting performance loss. Apparently, the BER curves are slightly flatter, demonstrating a small loss of diversity. This effect is less significant at higher bandwidths, where IPI is reduced [50].

In [53] the IPI has been investigated for PPM and TR modulation schemes. The authors call this interference cross-modulation interference (CMI) because it occurs between the waveforms used in the signaling schemes. Mitigation techniques against CMI have been developed, for coherent and noncoherent receivers. TR schemes have been presented in [54], [55], which can cancel the IPI by combining two consecutive pulse pairs with so-called "balanced" data encoding.

IPI also occurs within the pulse bursts used in the IEEE 802.15.4a signaling scheme [11]. It leads to a "code-induced" increase of fading, as analyzed in [56]. However, CMI between the BPPM positions is avoided, when using a sufficiently long burst position modulation interval T_{PPM}, see Figure 3(d).

POWER LIMIT CONSIDERATIONS, COMPLEXITY, AND IMPLEMENTATION ASPECTS

After illustrating performance tradeoffs with respect to system choices, the discussion is turned towards practical aspects influencing the system design. First, the allowed energy allocation to each transmitted symbol is addressed, considering the FCC's regulations for UWB systems [12]. It will be shown for low data rates that more energy can be transmitted by encoding data in several pulses. Second, the power consumption is studied of the components of a low-complexity ED receiver.

POWER LIMITS

In the regulations by the FCC [12], two different power limits have been defined. The average power is limited to -41.3 dBm/MHz. It is defined as the equivalent isotropic radiated power contained in a 1 MHz-band when averaged over a time window of $T_{\mathrm{Av}} = 1$ ms and maximized over the signal bandwidth B. Additionally, a peak power limit is defined, where the maximum power must not exceed 0 dBm after filtering with 50 MHz centered at the frequency with the highest emission level. The two constraints result in two different operating regimes [57]. This is illustrated in Figure 10(a) for a BPPM transmitter which modulates the pulse polarity by a random sequence. The figure shows the maximal FCC-compliant pulse energy with respect to the peak and average power constraint as a function of the pulse repetition rate R. To decouple the plot from pulse shape and bandwidth, an ideal transmit bandpass is assumed and the pulse energy is normalized to the two-sided pulse bandwidth $2B$. The maximal allowed pulse energy with respect to the average power constraint decreases linearly with pulse rate R, considering the random polarity modulation. The allowed pulse energy with respect to the peak power constraint stays unchanged up to a pulse rate of about $R = 75$ MHz and decreases quadratically at higher pulse rates [57].

In Figure 10, two operating regimes are identified. For pulse rates $R < 1$ MHz, the peak power constraint is much more restrictive than the average power constraint. It leads to an average transmit power that is well below the allowed level. To fully exploit both constraints at low data rates, [57] proposes to replace each pulse by a sequence of pulses that are temporally separated by the allowable $\tau_{\mathrm{Ref}} = 1/(75\ \mathrm{MHz})$. This increases the total radiated energy per symbol, while keeping the peak power constant. The technique has been called modified pulse repetition coding (MPRC). For $R < 1$

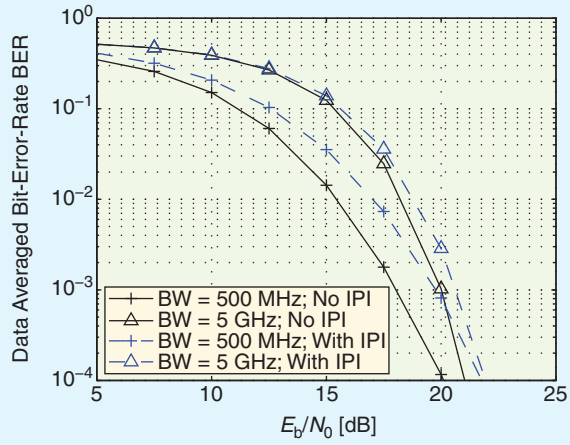

[FIG9] Performance of TR schemes at different bandwidths with small-scale fading and, optionally, with IPI between reference and data pulse.

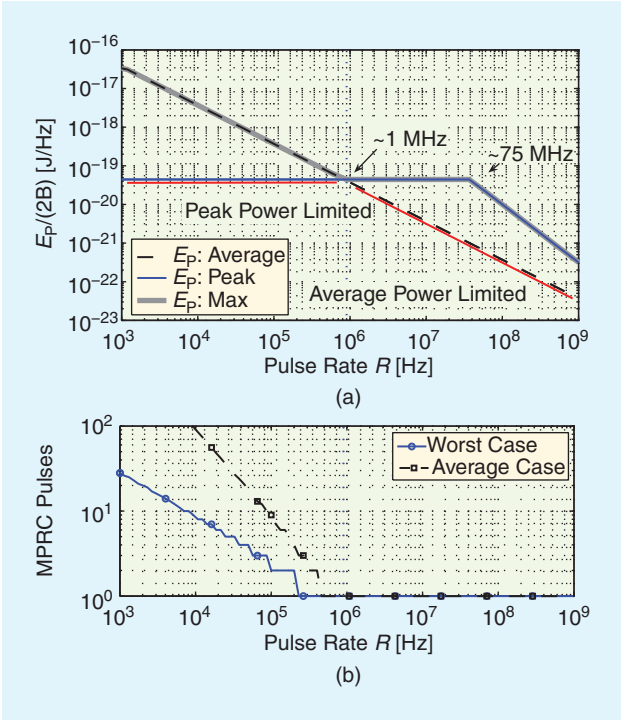

[FIG10] (a) Maximal FCC-compliant pulse energy with respect to peak and average power constraints, given as normalized pulse energy $E_p/(2B)$. (b) Maximum number of MPRC pulses.

MHz, the maximal FCC-compliant pulse energy achievable by MPRC is indicated by the bold, shaded line in Figure 10(a). Figure 10(b) indicates the corresponding number of maximal allowed MPRC pulses, which is determined again by the average power constraint. For symbol rates close to 1 kHz, the number of pulses is dictated by a worst case scenario, as no time averaging can be considered in $T_{Av} = 1$ ms. For higher rates, averaging effects occur and the maximal allowed number of pulses can be taken from a more relaxed average limit.

At pulse rates $R > 1$ MHz, the average power constraint is more restrictive. As shown in [58], this can be used to optimize low duty cycle systems, which are idle most of the time and active for brief periods only. With a proper balance of burst and idle times, the power of a burst can be maximized.

COMPLEXITY AND IMPLEMENTATION ASPECT

The low complexity of noncoherent receivers makes them very attractive for the use in wireless sensor and body area networks, where low power consumption is essential. In [58], a UWB-IR transceiver is presented which illustrates the high potential of noncoherent concepts for ultra-low-power applications. A rigorous application and hardware aware optimization of the system, which has been based on state-of-the-art UWB components described in the literature, facilitates a power consumption below 1 mW. The key to this low power consumption lies in the combination of a dominantly analog circuit design and a very low duty cycle operation at a high peak data rate. The low duty cycle allows to turn off the system during idles times. As the current consumption of the analog part is independent of the data rate, it scales with the duty cycle. The design in [58] operates at a 1% duty cycle by radiating bursts of 10 μs every 1 ms. With a peak data rate of 50 Mb/s and an average transmit power of -14.31 dBm at 500 MHz bandwidth, the transmitter is FCC compliant. It achieves an effective data rate of 500 kb/s.

The block diagram of the receiver chain is shown in Figure 11. Minimization of the relative bandwidth minimizes the complexity of the analog components. Hence a system bandwidth of 500 MHz has been chosen according to the FCC's minimum requirement for UWB [12]. To maximize the SNR, the noise is bandpass filtered after the low-noise amplifier (LNA). However, nonlinear characteristics of the LNA can cause in-band copies of the out-of-band interference. In this case, the bandpass filter should be shifted in front of the LNA, at the expense of a reduced SNR.

After the bandpass filter, the signal is amplified by a variable gain amplifier (VGA), controlled by a programmable gain

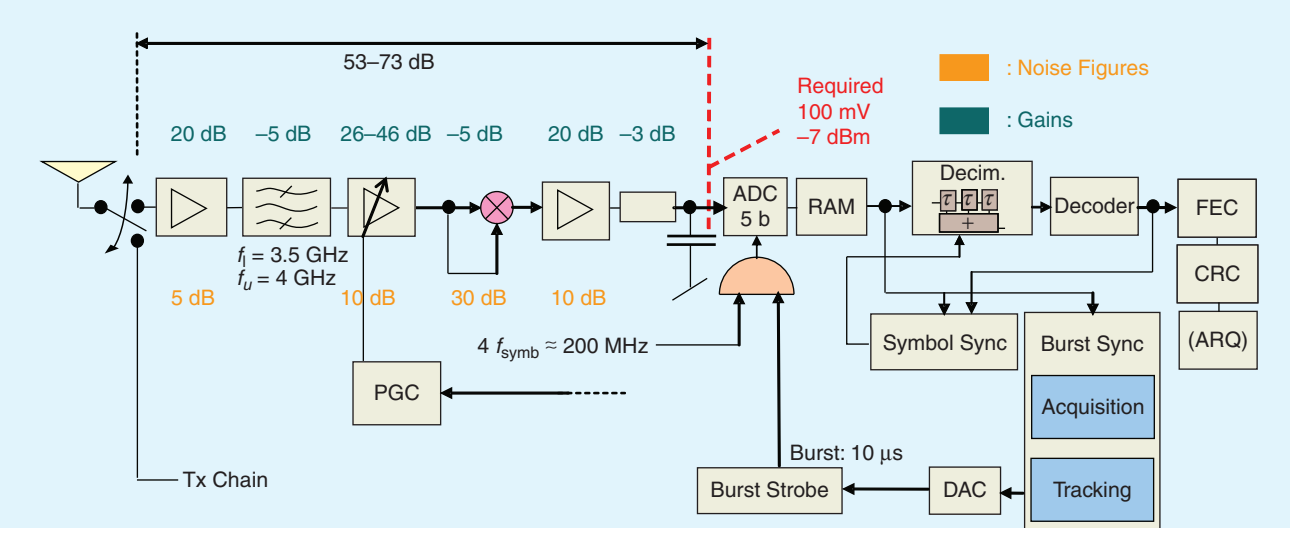

[FIG11] Block diagram of the UWB-IR receiver [58].

control (PGC), squared and amplified again by a third amplifier. In absence of interference, the required IIP3 points of the LNA and amplifiers can be very low. Finally, the signal is low-pass filtered and fed to an ADC. A simple first-order, low-pass filter is used as a replacement for standard integrators that are very power consuming [3]. The power gains and noise figures (NFs) of the individual analog components are indicated in Figure 11. These are typical values taken from literature. The PGC tunes the VGA between 26 and 46 dB such that the input amplitude to the ADC stays around 100 mV.

The ADC, together with a random access memory (RAM), builds the interface to the digital receiver part. To keep the ADC power consumption small its resolution is set to just 5 b. It is driven by a clock at four times the symbol rate, i.e., at 200 MHz. The RAM decouples the digital part from the symbol rate and allows burst-wise processing. Its output is fed to the burst and symbol synchronization blocks. Burst synchronization is realized by a pilot-based correlation approach that achieves synchronization after a single burst [59]. The symbol synchronization interpolates and down-samples the input signal and thus enables a free-running clock. After the decimator, the decoder consists of a simple subtraction. Forward error correction (FEC), cyclic redundancy check (CRC) code, and automatic repeat request (ARQ) control are not specified in the current proposal.

Based on expertise and state-of-the-art literature (see [58] and references therein), the current consumption of the LNA, amplifiers, sampling clock, mixer, and ADC are estimated to $I_{\mathrm{LNA}} = I_{\mathrm{Amp}} = I_{\mathrm{s}} = 5$ mA, $I_{\mathrm{Mix}} = 1.5$ mA and $I_{\mathrm{ADC}} = 3$ mA, respectively, when realized with 0.18 μm technology and a supply voltage of 1.8 V. At a 100% duty cycle, the overall current consumption of the analog receiver part results in $I_{\mathrm{Analog}} = I_{\mathrm{LNA}} + 2 \cdot I_{\mathrm{Amp}} + I_{\mathrm{Mix}} + I_{\mathrm{ADC}} + I_{\mathrm{s}} \approx 24.5$ mA. The analog current consumption scales with the duty cycle. That is, for a 1% duty cycle, the current consumption scales down to $I_{\mathrm{Analog}} \approx 0.25$ mA. The digital current consumption is estimated to $I_{\mathrm{Digital}} \approx 0.2$ mA [58] and is independent of the duty cycle. The overall receiver current consumption as a function of the duty cycle η is therefore given by $I_{\mathrm{Tot}}(\eta) = I_{\mathrm{Digital}} + \eta I_{\mathrm{Analog}}$, $\eta \in (0, 1)$. For $\eta = 1$, it equals $I_{\mathrm{Tot}} \approx 25$ mA, while at a duty cycle $\eta = 0.01$ the current consumption reduces to $I_{\mathrm{Tot}} \approx 0.45$ mA. This corresponds to a current saving of 98%.

The current consumption of a reference transmitter [3] is estimated around 0.04 mA at $\eta = 0.01$. With this, the overall transceiver power consumption is expected to be below 1 mW.

The discussed design has been based on components described in the literature, but the authors are not aware that any noncoherent UWB receiver chips are commercially available yet. Prototypes have been built using off-the-shelf radio frequency (RF) components. For instance, in [60], a prototype implementation according to the IEEE 802.15.4a standard is discussed, which employs an energy detector. Reference [61] describes a complementary metal–oxide–semiconductor (CMOS) implementation of a transmitter for this standard, which consumes about 1 mW at a data rate of 1 Mb/s.

RECEIVER SIGNAL PROCESSING

This section addresses the key signal processing tasks arising in the practical implementation of a noncoherent UWB receiver. Often, codesigns of signaling schemes, receiver architectures, and back-end processing techniques have been proposed to solve the challenges in the transceiver design.

SYNCHRONIZATION AND TIME-OF-ARRIVAL ESTIMATION

Relaxed synchronization requirements are a frequently stated advantage for the type of noncoherent UWB schemes discussed in this work (e.g., [2], [18], [28], [35]). As discussed above, a coherent receiver has to synthesize a template waveform corresponding to the UWB channel impulse response and, to avoid performance losses, align it to the incoming pulses at an accuracy that is by about an order of magnitude below the bandwidth reciprocal, typically in the range of tens of picoseconds. Considering clock and carrier jitter in low-cost, low-power hardware, this is extremely challenging.

Noncoherent receivers align their integration window to capture the energy of the UWB pulses as shown in the section "Signaling Schemes and Receiver Architectures." This requires much less accuracy and also allows a safety margin. The performance as a function of the integration window length, which has been reviewed in the section "Performance Comparison and Optimization," yields intuition on the accuracy requirement in this case. Notably, the curves are rather flat near the optimum (see Figure 6). A deviation of 10% off this optimum has negligible influence. Thus, a synchronization inaccuracy in the order of 10% of the window length would be acceptable. Typically, this requirement is in the nanosecond range.

The rest of this subsection is a literature overview on synchronization for noncoherent UWB systems. We do not illustrate any technique in detail, because this has already been elaborated in this magazine in [2].

Acquisition Schemes

Autocorrelation operations, similar to the AcR as described by (2), have been exploited in UWB to achieve synchronization acquisition. One example is introduced by Yang and Giannakis, called "timing with dirty templates" (TDT) [2], [62]. The idea relies on an autocorrelation operation among symbol-spaced segments (called "dirty templates") of the received UWB signal. Under certain circumstances, a maximum is obtained if the delay of the segments corresponds to the timing offset.

Synchronization acquisition for the delay-hopped transmitted-reference system by Hoctor and Tomlinson [10], see Figure 4(b), has been discussed in [63] and [64], where data-aided as well as nondata-aided schemes are proposed.

Fractional Sampling

Noncoherent UWB schemes can be operated without explicit synchronization of the integration interval. This is especially true for receivers that use fractional sampling (see

e.g., [41]–[43]). It has been suggested to weight these samples for performance optimization, as discussed in the section "Performance Enhancement." Such weighting, performed in the digital back-end of the receiver, implicitly accounts for timing offsets, because emphasis is given to the samples containing most energy. Another way to avoid explicit timing is to interpret mistiming as ISI and to deal with it through equalization [65].

The performance of synchronization schemes based on fractional sampling has been analyzed for instance in [3], [48], and [59]. However, an estimation of the propagation delay is only approximately possible because of the unknown channel impulse response. This limits the applicability of such techniques for high-precision ranging, but the accuracy is sufficient for a communication receiver.

Time-of-Arrival Estimation with Noncoherent Receivers

Time-of-arrival (ToA) estimation for ranging and localization is very closely related to synchronization techniques, as it requires the estimation of the signal arrival time. To achieve an accuracy in the order of a nanosecond, the receiver has to sample the received UWB pulse envelope at Nyquist rate, even with noncoherent receiver front ends. However, unlike with coherent receivers, the sampling rate can be reduced by increasing the integration interval, if a reduced accuracy can be tolerated [66].

A variety of leading edge detectors can be applied to the acquired energy samples of the received UWB pulses, as described in [67]. It concludes that the search-back approach, which identifies the first relevant multipath component preceding the maximum component within a certain window, performs best at low- to medium-SNR.

A ranging performance comparison of coherent and noncoherent receivers can be found in [68]. Clearly, the noncoherent schemes are worse in exploiting averaging, due to the noise-by-noise crossterm (see the performance results in the section "Performance Evaluation"). On the other hand, especially at sub-Nyquist sampling rates, noncoherent schemes are more robust to timing errors.

High-accuracy indoor ranging and positioning has been the main motivation to propose the UWB-based standard known as IEEE 802.15.4a [11]. Perhaps the most unique element of the standardized transmission scheme in the context of ranging is the definition of a ternary preamble code for synchronization and ToA estimation, which has special autocorrelation properties that can be exploited by noncoherent receivers [69].

NARROWBAND INTERFERENCE MITIGATION

Narrowband interference (NBI) is a fundamental problem for noncoherent UWB receivers, foremost because the signal-to-interference ratio at the receiver antenna can be very low. Evidently, a notch filter can be used to reduce such interference, but firstly the suppression of a receiver front-end filter could be insufficient, secondly the notch frequency should be adaptable to be optimal, and thirdly more than one narrowband interferer could be present.

A number of research papers have addressed the NBI problem in the context of noncoherent receiver architectures. Performance and SINR analyses in presence of NBI are found in [70]–[72] for autocorrelation receivers and in [73] and [74] for EDs. In most of these references, mitigation schemes have also been proposed, based on the characteristics of the interfering signals. This section develops intuition for the NBI problem and the proposed mitigation techniques.

NBI Modeling

The NBI signal at the receiver input can be modeled as a bandlimited (Gaussian) noise process

$$\beta(t) = \sqrt{2}\,\Re\{\alpha(t)e^{j(2\pi f_\beta t+\theta)}\}$$

at carrier frequency f_β, which is expressed by its complex-valued envelope $\alpha(t)$. Its autocorrelation function is modeled as

$$\begin{aligned} R_{\beta\beta}(\tau) &= \mathrm{E}\{\beta(t+\tau)\beta(t)\} \\ &= P_\beta \cos(2\pi f_\beta \tau)\,\mathrm{sinc}(W_\beta \tau), \end{aligned}$$

where P_β denotes the signal power and W_β the bandwidth.

Assume the desired UWB signal, the NBI signal, and a noise signal are present at the input of an energy detection front end (1) or an AcR (2). Then, nine product terms comprise the output samples due to the nonlinear operations. Most mitigation schemes focus on the NBI-by-NBI coterm, among these contributions, which can be written for a generic AcR branch with delay D_n (including the ED where $D_n = 0$) as

$$\begin{aligned} \beta_n[i] &= \int_{t_{i,n}}^{t_{i,n}+T_\mathrm{I}} \beta(t+D_n)\beta(t)dt \\ &= \int_{t_{i,n}}^{t_{i,n}+T_\mathrm{I}} \Re\{\alpha(t+D_n)\alpha(t)\}\cos[2\pi f_\beta(2t+D_n)+2\theta]dt \\ &\quad + \cos(2\pi f_\beta D_n)\int_{t_{i,n}}^{t_{i,n}+T_\mathrm{I}} \Re\{\alpha(t+D_n)\alpha^*(t)\}dt. \end{aligned} \tag{11}$$

This result can be further simplified, if the coherence time of the NBI (approximately $1/W_\beta$) is considerably larger than T_I, which is a reasonable assumption in the UWB case. This allows us to take the $\Re\{\cdot\}$-terms out of the integrals and rewrite them as $\tilde{\varphi}_\alpha(t_{i,n}, D_n)$ and $\varphi_\alpha(t_{i,n}, D_n)$, such that

$$\beta_n[i] = \tilde{\varphi}_\alpha(t_{i,n}, D_n)\int_{t_{i,n}}^{t_{i,n}+T_\mathrm{I}} \cos[2\pi\, f_\beta(2t+D_n)+2\theta]dt \tag{12}$$

$$+\ \varphi_\alpha(t_{i,n}, D_n)T_\mathrm{I}\cos(2\pi\, f_\beta D_n). \tag{13}$$

The integral in (12) depends on the actual sampling times $t_{i,n}$ of the receiver front end and also on the phase θ of the NBI. Its magnitude is determined by the length of the integration window T_I in relation to the NBI frequency f_β. If $2f_\beta T_\mathrm{I}$ is an integer value, then it spans a full number of cosine cycles, such that (12) is zero. Therefore, adaption of the integration window can be used to reduce or cancel this interference term, assuming f_β is known.

However, (13) will be dominant by far in most cases, because $T_\mathrm{I}\cos(2\pi f_\beta D_n)$ is considerably larger than the integral

in (12); see [70]. The term (13) is a (time-variant) bias in the receiver output, depending on the magnitude of the envelope $\alpha(t)$ through $\varphi_\alpha(t_{i,n}, D_n)$ and on the correlation lag D_n through $\cos(2\pi f_\beta D_n)$. By proper choice of D_n, the term could be made zero, assuming f_β is known.

Therefore, a range of mitigation schemes has been proposed to reduce the latter term [70], [72], [73], [75]. The work by Steiner and Wittneben [73] demonstrates a natural resilience of BPPM signaling with energy detection against this interference. Subtracting two consecutive samples for BPPM detection implies that the interference is cancelled, if both samples are taken well within the coherence time of the NBI signal; that is if $\varphi_\alpha(t_{i,n}, D_n = 0)$ can be considered constant for two consecutive sampling instants $t_{i,n}$. The processing gain of BPPM and, as reference, the processing gain of an optimal coherent receiver are shown in Figure 12. The figure reveals that the inherent NBI resilience (processing gain) of BPPM detection quickly decreases with increasing NBI bandwidths, when a noncoherent detector is employed.

Based on the same approach, a code design has been suggested in [70] for transmitted-reference modulation. In this scheme, each data symbol is encoded in two consecutive pulse pairs such that the decision variable is obtained from subtracting two corresponding consecutive receiver samples. Thereby, the NBI term (13) is cancelled, if both samples are acquired within its coherence time. In [75], a signal processing scheme is developed, which is also based on the assumption of coherence of the NBI over a number of consecutive samples. The NBI component can be identified in the data and suppressed.

A different approach has been proposed in [72] to suppress NBI for AcR and ED receivers. Here, multiple parallel AcR front ends provide samples of $\beta_n[i]$, (11), at various correlation lags $\{D_n\}$, in which the NBI contribution can be identified and suppressed. Consider (13). If the range of lags $\max\{D_n\} - \min\{D_n\}$ does not exceed the coherence time of the NBI, all $\varphi_\alpha(t_{i,n}, D_n)$ are approximately equal. Hence the dominant NBI term appears as a sampled cosine waveform, which can be easily identified in the data and suppressed. Up to 50 dB gain in terms of signal-to-interference ratio has been reported in [72], using an eight-channel AcR front end.

So far, the discussion has neglected any of the other product terms arising in the AcR and ED. The variance of the NBI-by-UWB cross term, for instance, depends on the product of the NBI power and the power spectral density of the UWB pulse at the NBI frequency [70], [72]. Therefore it will be of little concern to out-of-band interferers, and it can be mitigated by spectral shaping. It is normally much weaker than the NBI-by-NBI coterm, but it could become of relevance if the coterm is well suppressed. In this case, the cross-term should be mitigated as well. In [70], a proper choice of the symbol duration as a function of the NBI frequency is suggested. Thereby the interference components are made equal in consecutive samples. Subtracting these samples to compute the decision variables thus cancels the NBI cross-term. In [73], the time duration of the UWB pulse is adjusted to the NBI in order to produce spectral zeros at f_β. This can be seen as low complexity spectral shaping.

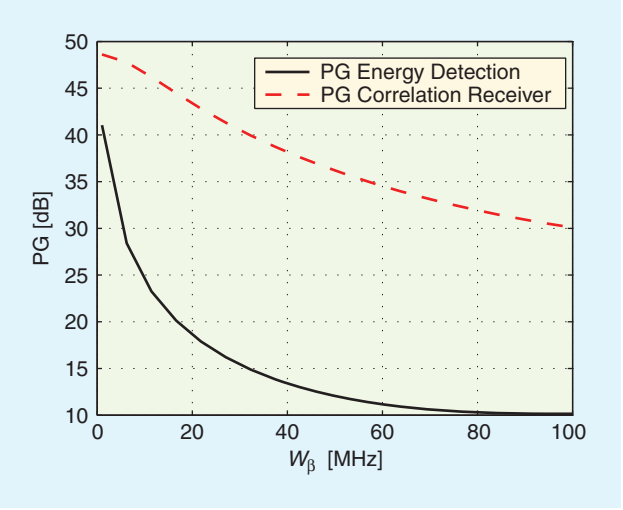

[FIG12] Processing gain (PG) of a noncoherent BPPM detector against narrowband interference, compared with a coherent receiver [73].

The work in [72] demonstrates that the multichannel AcR also provides information about this cross-term, such that it can be efficiently mitigated. Surprisingly, the same holds for the NBI-by-noise cross-term. This insight is supported by the analysis in [76], which elaborates that multiple parallel AcRs allow for the reconstruction of the power spectrum of the received signal. Hence, nulling the NBI frequency also nulls any NBI cross-terms at the NBI frequency.

Frequency selective preprocessing of the UWB signal is another approach that has been suggested by several authors for NBI suppression. In [77], a frequency-channelized parallel autocorrelation receiver has been analyzed. Skipping affected frequency bands, NBI can be avoided at the loss of some signal power. In [78], an architecture has been described with quadrature downconverters to bring the NBI signal to the baseband and to suppress the NBI there with fixed lowpass filters. The performance of the filtering approach has also been analyzed in [79], but without suggesting an actual implementation of the suppression filter. The filtering approach has the great advantage that it may avoid saturation of the receiver LNA. In the post-processing schemes discussed before, LNA saturation is eased by the fact that the peak-to-average power ratio of a UWB signal may be extremely high due to the signal sparsity. Therefore, small ratios of signal-to-interference power are possible at identical peak signal amplitudes.

Finally, [80] introduces a feedback loop with a symbol-length delay for reference pulse averaging, to enhance the signal-to-interference ratio of the template in a TR system. This approach inherently suffers from the danger of amplifying the NBI, if the delay is an integer multiple of the NBI signal period. From an implementation point of view, it could be hard to realize the required delay line.

EQUALIZATION AND HIGH-RATE NONCOHERENT UWB

The dispersive nature of the multipath propagation channel leads to ISI, when the symbol duration of the transmitted signal

approaches the channel delay spread. To combat ISI, equalization schemes or parallel transmission concepts like orthogonal frequency-division multiplexing (OFDM) can be used. In traditional radio communication systems, it is common practice to model the ISI as a linear finite-impulse response (FIR) filter, since the radio channel and system components are (virtually) linear. Based on this linear model, numerous equalization approaches have been developed, including linear (inverse) filters, decision feedback schemes, and (ML) sequence estimators [30].

A fundamental difference appears, when we investigate the (equivalent) system model of a noncoherent UWB system according to Figure 2. The radio channel is still linear. However, following the front-end filter, severely nonlinear operations are performed in the receiver front end: the energy detection or the autocorrelation operation. The result is nonlinear ISI, which can be modeled as a second-order Volterra system, written as [22]

$$y[i] = h_0 + \sum_{n=0}^{N} h_{1,n} d[i-n] + \sum_{n=0}^{N} \sum_{m=n+1}^{N} h_{2,n,m} d[i-n] d[i-m] + \nu[i]. \quad (14)$$

This model relates the data symbols $d[i]$ to the output samples $y[i]$ of the noncoherent receiver front end. The coefficient h_0 is a bias term, the coefficients $\{h_{1,n}\}$ represent a linear FIR system, and the coefficients $\{h_{2,n,m}\}$ stand for a second-order nonlinear FIR system, accounting for the cross products among all combinations of data symbols. Finally, an additive noise term $\nu[i]$ is introduced, which accounts for the noise-by-noise coproduct as well as the data-by-noise cross-term. This model has been derived for (delay-hopped) transmitted-reference UWB systems, but also holds for energy-detection receivers (see [42]).

The equivalent model (14) has been the basis of several works on equalization schemes for differential UWB systems [22], [42], [81]. In [22] and the references therein, it has been shown that the nonlinear terms of the data model can be incorporated in ML sequence detectors, which leads to efficient suppression of ISI-induced error floors. Linear and nonlinear FIR equalizers based on symbol-spaced samples have been investigated in [81]. In [42], fractional sampling of the receiver output has been discussed, resulting in a multiple-output Volterra model. In such a system, the nonlinear components can be interpreted as a linear interference signal that can be suppressed by linear processing schemes.

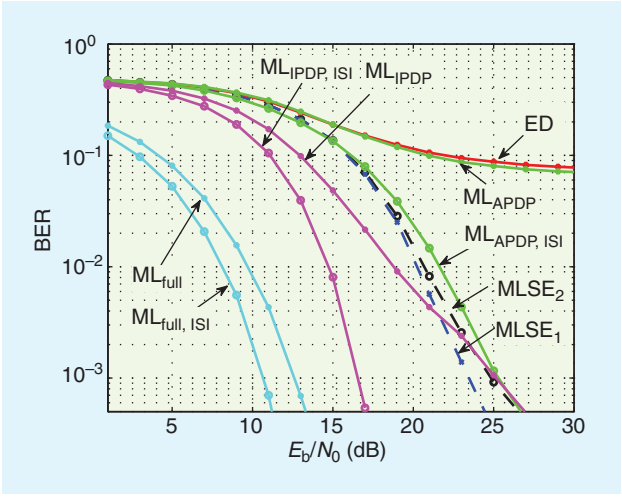

[FIG13] BER curves of BPPM transmission schemes under strong ISI [46]. The transmission rate is 50 Mb/s and the channel impulse response has a duration of 17 ns with a rectangular average power delay profile.

The equalization schemes discussed above require training to accurately estimate the coefficients of the Volterra system. A multiple symbol differential detection scheme for differential signaling has been derived in [82], based on the generalized likelihood ratio test (GLRT), which includes an estimation of channel state information. The resulting detector computes in its front-end autocorrelation operations among symbol-long segments of the received signal, whereas in the back-end, the Viterbi algorithm or sphere decoding can be applied to obtain a powerful detector. Remarkably, the GLRT derivation leads to a system architecture with an AcR in the front end.

A comprehensive study of low-complexity BPPM schemes under weak to moderate ISI is found in [46], where the memory length $N \leq 1$ (less than one symbol). The authors first derive symbol-wise ML detectors, assuming the availability of channel state information (CSI) to various degrees. A performance comparison is depicted in Figure 13. Full knowledge of CSI yields in absence of ISI the matched-filter receiver, which is shown for reference. Additional gain is possible, if ISI is taken into consideration and full CSI knowledge is assumed. Drops in performance are obtained if the instantaneous power delay profile (IPDP) or the average power delay profile (APDP) are assumed to be known. No knowledge of CSI leads to the ED, whose performance can be improved by using the Viterbi algorithm [maximum-likelihood sequence estimator (MLSE)] in the back-end; with ($MLSE_1$) or without ($MLSE_2$) taking nonlinear ISI crossterms into account, see (14).

Note that the performance gap increases clearly between coherent and noncoherent receivers, compared with results in absence of ISI. It is in the order of 12–15 dB in Figure 13, comparing the ED with MLSE and the best coherent receiver $ML_{full, ISI}$. But the gap is only about 5–8 dB in a comparison without ISI (see Figure 8 and [46]).

In [83], decision feedback equalizers are considered for on-off keying systems. A linear system model is derived, which only considers a memory length of one, however.

Parallel multicarrier transmissions are an alternative approach to increasing the data rate. It is well known from the OFDM concept that ISI can be avoided in such a setup, since the symbol rate on each subcarrier is significantly reduced. In a noncoherent setup, the front end contains parallel bandpass filters to separate the frequency carriers and to perform OOK or BPPM detection separately on each channel [84]. Integration of the bank of highly selective bandpass filters is probably the key problem of this approach. The implementation study in [85] unfortunately does not comment on this issue and [86] shows

simulation results only. An alternative receiver architecture has been suggested in [76], which employs a bank of AcRs in the receiver front end. A Fourier transform in the back-end yields an estimate of the energy spectrum of the input signal, which can be used for detecting the energy of the subband signals.

The tradeoff between multicarrier transmission and equalization has been investigated in [87]. Various performance and complexity tradeoffs are discussed. More fading remains in a four-channel scheme compared with a single-carrier approach. When applying in addition FEC, the four-channel scheme is able to exploit the full diversity of the channel. Consequently, the multicarrier receiver performs favorably at lower complexity when error correction coding is considered.

MULTIPLE ACCESS

Low-data-rate IR-UWB systems are spread spectrum systems that inherently support a large number of users. This can easily be understood by considering its processing gain. As for traditional "narrowband" systems, the processing gain for UWB systems is approximately $2WT$, where W is the signal bandwidth and T is the symbol period. In the UWB case, the processing gain exceeds 1,000, assuming a data rate below 1 Mb/s and a bandwidth above 500 MHz. This indicates the multiple access support of a very large numbers of users (see [14] and [15]), without the need of any (time) harmonization between the IR-UWB transmitters. In other words, IR-UWB-transmitters may transmit at will without interfering too much with the others. This reduces the multiaccess control overhead significantly.

IR can be thought of as a specialization of direct-sequence spread spectrum (DSSS). Instead of using an antipodal DSSS code, IR uses codes containing ones and zeros, in which the zero occurs significantly more frequent than the one. A pulse is only transmitted when the code value is equal to one resulting in a sparse signal. For a complete description of the code, only the relative time position of the ones need to be defined and is therefore referred to as a TH code.

Due to their sparsity, the probability of two different TH codes having an inner-product other than zero is small, making IR less susceptible to the near-far effect. Signal orthogonality results from the sparsity in the time domain, instead of in the code domain [14]. Also the receiver complexity is reduced; only the sparsely received pulses need to be processed, in contrast to the demanding de-spreading operation of a highly spread DSSS signal. Nevertheless, IR can be seen as a specialization of DSSS systems and their processing gains are interchangeable [88].

Unfortunately, the high spreading gains are not obtained when noncoherent receivers are employed. The reason lies in the signal processing operations performed in the receiver front end. An optimal receiver projects the received signal onto the transmit code subspace, which is a small subspace in the multidimensional signal space of UWB signals. Noncoherent receivers cannot perform this projection due to their front-end architecture. Only timing information can be exploited in ED receivers, while AcRs project the signal onto a (random) basis that is corrupted by noise and interference.

As introduced in the section "Signaling Schemes and Receiver Architectures," combinations of TH and delay hopping have been suggested as multiple access schemes for noncoherent UWB schemes. In TH schemes [14] and [15], see Figure 3(c) and (d), the despreading operation is limited to the selection of the integration intervals, which suppresses the interfering signal at all other times [see Figure 3(c)]. Delay hopping can be used with TR systems, where the delays of the AcRs are matched to the spacings between the reference and data pulses [10], [21]; see Figure 4(b) and (d).

In the above-described multiple access schemes, the main despreading operation is performed in the analog front end, in some cases in conjunction with back-end signal processing to combine the acquired energy samples and account for an amplitude code (e.g., [10]). This will be the setup for a low-complexity multiple-access UWB system. There are few papers evaluating the performance of such systems. For the TR signaling principle, a semi-analytic approach has been developed in [21]. A Gaussian approximation has been employed for the MAI, whose variance is expressed for a given set of channel realizations. Conventional TR modulation, using explicit reference pulses, has been compared to the frame-differential signaling scheme, see Figure 4(b) and (d), respectively. In both cases, each user is assigned a (set of) specific delay(s) for its AcR(s). It has been found that the multiple access capacity is approximately doubled for the frame-differential scheme, which only employs a single pulse per frame. The TR system needs two pulses per frame and hence produces twice the amount of MAI. Around 80 and 40 users, respectively, are supported at 1 Mb/s at a signal bandwidth of about 4 GHz, when a single frame per symbol is employed. In a perfect coherent system at comparable specifications, the number of users could be in the hundreds or even thousands [15].

Reference [21] also addresses the impact of the number of pulses per symbol. Figure 14 illustrates the performance of two 100 kb/s systems at 4 GHz bandwidth, one using $N_s = 1$ and the second one using 20 pulses per symbol. As discussed in the

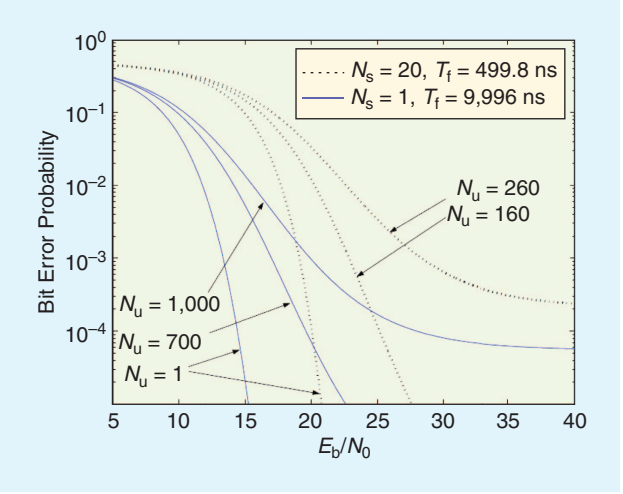

[FIG14] Multiple-access performace comparison for frame-differential TR systems [21].

section "Performance Comparison and Optimization," the single-pulse system clearly outperforms the multipulse system in the single user case ($N_u = 1$). But the number of supported users is also higher in the single-pulse case, where up to $N_u = 1{,}000$ users seem feasible, although there is a certain risk that the signals of two users interfere completely in this case. The main drawback for the considered single-pulse system is the required delay line at $\approx 10\ \mu$s and 4 GHz bandwidth, which can only be implemented digitally. (Reference [89] discusses an inaccuracy in [21]. It is unlikely that this affects the general conclusions discussed here, but the absolute results may be inaccurate.)

The investigations in [90] illustrate the nonlinear components in the signal model of a multiple access scenario with AcR detection, which is similar to the ISI signal model discussed in the section "Equalization and High-Rate Noncoherent UWB." Crossproducts between the users' data have to be considered. The article demonstrates the effectiveness of MLSE for this case.

Enhanced detectors for symbol-differential UWB systems, see Figure 4(c), have been investigated in [82], in presence of MAI. The detectors are based on multisymbol differential detection and employ a coherent combiner prior to the AcR, which is matched to the TH code. (Note that this preprocessing is similar to the hybrid matched filter architecture of [18].) They show excellent resilience against MAI, with satisfactory performance in scenarios of up to $N_u = 100$ users at 400 kb/s.

Another scheme with pre-AcR averaging has been proposed in [91]. The authors assign a pair of signature sequences to the reference and data pulses to suppress MAI by coherent combining. A similar principle is exploited in [38], where the template signal for the AcR detection is derived from multiple pilot signals. A performance evaluation has been given for a 50-user environment, where MAI has been modeled as Gaussian noise. The work in [89] introduces a so-called balanced TR scheme for multiple access, which cancels IPI by precoding data on consecutive TR frames. Simple post-processing is applied to the AcR output samples. The authors claim to achieve an MA capacity comparable to the conventional TR scheme, however at higher data rates.

TH multiple access for noncoherent ED has been integrated in the standardized IEEE 802.15.4a signaling scheme [11]; see Figure 3(d). It is also described in the textbook by Molisch [92], in the variant illustrated in Figure 3(c). Nevertheless, to the authors' knowledge, there is hardly any literature analyzing the multiple access capacity of this approach. In [93], the performance of such a system with PPM is investigated. The tradeoff is highlighted between the number of pulses per symbol and the number of TH frames. An error floor of around 1% has been obtained in a 30-user setup, using a signaling scheme with five pulses per symbol and 20 TH frames per pulse.

CONCLUSIONS AND OUTLOOK

An elaborate overview of recent advances in noncoherent UWB system design has been given, including practical implementation aspects, system design tradeoffs, and signal processing schemes. Noncoherent schemes typically lose some 5 dB or more of SNR with respect to optimal coherent receivers. On the other hand, they are far less vulnerable to time-variant multipath effects, phase jitter, synchronization offsets, and incomplete energy capture, such that this performance penalty could diminish in practice. On top of that, their implementation complexity is drastically reduced, because they don't require Nyquist-rate sampling of the received UWB signals. For these advantages, the authors expect to see an increasing number of implemented noncoherent UWB systems over the next years and a continued interest of the international research community in this topic.

ACKNOWLEDGMENT

The work of Geert Leus was supported in part by STW under the Green and Smart Process Technologies Program (Project 7976).

AUTHORS

Klaus Witrisal (Witrisal@tugraz.at) received the Dipl.-Ing. degree in electrical engineering from Graz University of Technology, Austria, in 1997, the Ph.D. degree (cum laude) from Delft University of Technology, The Netherlands, in 2002, and the Venia Docendi (Habilitation) from Graz University of Technology in 2009. From 1997 to 2001, he was a Ph.D. student and research engineer at Delft University of Technology. Currently, he is an associate professor at the Signal Processing and Speech Communication Laboratory (SPSC) of Graz University of Technology. His research interests are in signal processing for broadband and UWB wireless communications, propagation channel modeling, and positioning. He is cochair of the MTT/COM Society of the IEEE Austria Section.

Geert Leus (g.j.t.leus@tudelft.nl) received the electrical engineering degree and the Ph.D. degree in applied sciences from the Katholieke Universiteit Leuven, Belgium, in 1996 and 2000, respectively. Currently, he is an associate professor of electrical engineering, mathematics, and computer science at Delft University of Technology, The Netherlands. From March 2001 to May 2002 he was a visiting researcher and lecturer at the University of Minnesota. He received a 2002 IEEE Signal Processing Society Young Author Best Paper Award and a 2005 IEEE Signal Processing Society Best Paper Award. He is the chair of the IEEE Signal Processing for Communications Technical Committee and an associate editor for *IEEE Transactions on Signal Processing* and *EURASIP Journal on Applied Signal Processing*. His research interests are in the area of signal processing for communications.

Gerard J.M. Janssen (g.j.m.janssen@tudelft.nl) received the M.Sc.E.E. degree from Eindhoven University of Technology in 1986, and the Ph.D. degree from Delft University of Technology in 1998, both in The Netherlands. In 1986, he joined the Physics and Electronics Laboratory of the Dutch Organization of Applied Scientific Research (TNO), where he was involved in radar-cross-section modeling, radio direction finding, interference cancellation, and wideband propagation measurements. He is an associate professor with the Wireless and Mobile Communications group at Delft University of

Technology. His research interests are in wireless communication, especially narrowband multiuser detection, digital modulation techniques, channel modeling, diversity techniques, and ultra-wideband communications and positioning.

Marco Pausini (marco.pausini@gmail.com) received the Dr. Eng. degree in telecommunications engineering from the University of Bologna, Italy, in 2001 and the Ph.D. degree (*cum laude*) from Delft University of Technology, The Netherlands, in 2007. In 2007, he joined Verigy (formerly Agilent Technologies), Stuttgart, Germany, where he has been working as a R&D RF engineer. Since August 2008, he has been a physical layer engineer at AT4 Wireless, Malaga, Spain. His research interests are in the area of digital communications, with special emphasis on ultra-wideband and upcoming 4G wireless systems.

Florian Troesch (florian.troesch@nari.ee.ethz.ch) received his Dipl. El.-Ing. degree in electrical engineering from ETH Zurich, Switzerland, in 2003. Currently, he is research assistant at the Communication Technology Laboratory (CTL), ETH Zurich and is working toward his Ph.D. degree. His main research interests lie in the area of wireless communications with focus on low-power ultra-wideband systems.

Thomas Zasowski (thomas.zasowski@swisscom.com) received the Dipl.-Ing. degree in electrical engineering from Saarland University, Saarbrücken, Germany, in 2002. In 2007, he obtained the Dr. Sc. ETH degree from ETH Zurich, Switzerland. After finishing his Ph.D. dissertation in the area of UWB body area networks, he stayed as a postdoctoral researcher at the Communication Technology Laboratory (CTL), ETH Zurich, where he was leader of the UWB group. In 2008, he joined Swisscom Strategy & Innovation, Switzerland, where he works on future wireless communication systems.

Jac Romme (romme@imst.de) received the M.Sc. degree in electrical engineering from Eindhoven University of Technology in 2000 and the Ph.D. degree from Graz University of Technology in 2008. Since September 2000, he has been working as a research engineer at IMST GmbH, Kamp-Lintfort, Germany. He has been involved in various UWB projects on localization and data communication, among which are the IST FP5 project Whyless.com, the NRW project Puls-On, the IST FP6 project Pulsers 2, and the IST FP7 project UCELLS. His research interests are statistical signal processing, nonlinear detectors, channel equalization, and forward error control.

REFERENCES

[1] M. Z. Win and R. A. Scholtz, "Impulse radio: How it works," *IEEE Commun. Lett.*, vol. 2, no. 2, pp. 36–38, Feb. 1998.

[2] L. Yang and G. Giannakis, "Ultra-wideband communications: An idea whose time has come," *IEEE Signal Process. Mag.*, vol. 21, no. 6, pp. 26–54, Nov. 2004.

[3] L. Stoica, A. Rabbachin, H. Repo, T. Tiuraniemi, and I. Oppermann, "An ultra-wideband system architecture for tag based wireless sensor networks," *IEEE Trans. Veh. Technol.*, vol. 54, no. 5, pp. 1632–1645, Sept. 2005.

[4] M. Z. Win and R. A. Scholtz, "Characterization of ultra-wide bandwidth wireless indoor channels: A communication-theoretic view," *IEEE J. Select. Areas Commun.*, vol. 20, no. 9, pp. 1613–1627, Dec. 2002.

[5] A. Molisch, "Ultrawideband propagation channels—Theory, measurement, and modeling," *IEEE Trans. Veh. Technol.*, vol. 54, no. 5, pp. 1528–1545, Sept. 2005.

[6] M. K. Simon and M.-S. Alouini, *Digital Communication over Fading Channels*, 2nd ed. Hoboken, NJ: Wiley, 2005.

[7] J. Choi and W. Stark, "Performance of ultra-wideband communications with suboptimal receivers in multipath channels," *IEEE J. Select. Areas Commun.*, vol. 20, no. 9, pp. 1754–1766, Dec. 2002.

[8] C. Rushforth, "Transmitted-reference techniques for random or unknown channels," *IEEE Trans. Inform. Theory*, vol. 10, no. 1, pp. 39–42, Jan. 1964.

[9] R. Scholtz, "The origins of spread-spectrum communications," *IEEE Trans. Commun.*, vol. 30, no. 5, pp. 822–854, May 1982.

[10] R. Hoctor and H. Tomlinson, "Delay-hopped transmitted-reference RF communications," in *Proc. IEEE Conf. Ultra Wideband Systems and Technologies, UWBST*, Baltimore, MD, May 2002, pp. 265–270.

[11] *802.15.4: Wireless Medium Access Control (MAC) and Physical Layer (PHY) Specifications for Low-Rate Wireless PANs,* IEEE P802.15.4a-2007 (Amendment 1) Std., 2007.

[12] FCC, "Revision of part 15 of the commission's rules regarding ultra-wideband transmission systems," Federal Communications Commission (FCC), First Report and Order, ET Doc. 98-153, FCC 02-48, Adopted: Feb. 14, 2002, Released: Apr. 22, 2002.

[13] D. Dahlhaus, "Post detection integration for ultra-wideband systems with binary orthogonal signaling," in *Proc. IEEE Int. Conf. Ultra-Wideband, ICU*, Sept. 2005, pp. 136–141.

[14] R. A. Scholtz, "Multiple access with time-hopping impulse modulation," in *Proc. Military Communications Conf., MILCOM*, Oct. 1993, pp. 164–175.

[15] M. Z. Win and R. A. Scholtz, "Ultra-wide bandwidth time-hopping spread-spectrum impulse radio for wireless multiple-access communications," *IEEE Trans. Commun.*, vol. 48, no. 4, pp. 679–691, Apr. 2000.

[16] F. Troesch, F. Althaus, and A. Wittneben, "Modified pulse repetition coding boosting energy detector performance in low data rate systems," in *Proc. IEEE Int. Conf. Ultra-Wideband, ICU*, Sept. 2005, pp. 508–513.

[17] J. Romme and K. Witrisal, "Analysis of QPSK transmitted-reference systems," in *Proc. IEEE Int. Conf. Ultra-Wideband, ICU*, 2005, pp. 502–507.

[18] F. Tufvesson, S. Gezici, and A. Molisch, "Ultra-wideband communications using hybrid matched filter correlation receivers," *IEEE Trans. Wireless Commun.*, vol. 5, no. 11, pp. 3119–3129, Nov. 2006.

[19] A. D'Amico and U. Mengali, "GLRT receivers for UWB systems," *IEEE Commun. Lett.*, vol. 9, no. 6, pp. 487–489, June 2005.

[20] M. Ho, V. S. Somayazulu, J. Foerster, and S. Roy, "A differential detector for an ultra-wideband communications system," in *Proc. IEEE Vehicular Technology Conf., VTC*, Spring 2002, pp. 1896–1900.

[21] Y.-L. Chao and R. A. Scholtz, "Multiple access performance of ultra-wideband transmitted reference systems in multipath environments," in *Proc. IEEE Wireless Communications and Networking Conf., WCNC*, Atlanta, GA, Mar. 2004, pp. 1788–1793.

[22] K. Witrisal, G. Leus, M. Pausini, and C. Krall, "Equivalent system model and equalization of frame-differential impulse radio UWB systems," *IEEE J. Select. Areas Commun.*, vol. 23, no. 9, pp. 1851–1862, Sept. 2005.

[23] B. Analui and A. Hajimiri, "Statistical analysis of integrated passive delay lines," in *Proc. IEEE Custom Integrated Circuits Conf.*, Sept. 2003, pp. 107–110.

[24] D. Goeckel and Q. Zhang, "Slightly frequency-shifted reference ultra-wideband (uwb) radio," *IEEE Trans. Commun.*, vol. 55, no. 3, pp. 508–519, Mar. 2007.

[25] H. Xu, L. Yang, and D. Goeckel, "Digital multi-carrier differential signaling for UWB radios," in *Proc. IEEE Global Telecommunications Conf., GLOBECOM*, Nov. 2006, pp. 1–5.

[26] A. D'Amico and U. Mengali, "Code-multiplexed UWB transmitted-reference radio," *IEEE Trans. Commun.*, vol. 56, no. 12, pp. 2125–2132, Dec. 2008.

[27] S. Dubouloz, B. Denis, S. de Rivaz, and L. Ouvry, "Performance analysis of LDR UWB non-coherent receivers in multipath environments," in *Proc. IEEE Intern. Conf. Ultra-Wideband, ICU*, Sept. 2005, pp. 491–496.

[28] T. Q. S. Quek and M. Z. Win, "Analysis of UWB transmitted-reference communication systems in dense multipath channels," *IEEE J. Select. Areas Commun.*, vol. 23, no. 9, pp. 1863–1874, Sept. 2005.

[29] M. Pausini, "Autocorrelation receivers for ultra wideband wireless communications," Ph.D. dissertation, Delft Univ. of Technology, Delft, The Netherlands, Dec. 2007.

[30] J. G. Proakis, *Digital Communications*, 2nd ed. New York: McGraw-Hill, 1995.

[31] P. Humblet and M. Azizoğlu, "On the bit error rate of lightwave systems with optical amplifiers," *J. Lightwave Technol.*, vol. 9, no. 11, pp. 1576–1582, Nov. 1991.

[32] S. Franz and U. Mitra, "Generalized UWB transmitted reference systems," *IEEE J. Select. Areas Commun.*, vol. 24, no. 4, pp. 780–786, Apr. 2006.

[33] F. Troesch and A. Wittneben, "An ultra wideband transmitted reference scheme gaining from intersymbol interference," in *Proc. Asilomar Conf. Signals, Systems, and Computers*, Nov. 2007, pp. 1070–1074.

[34] Y. Na and M. Saquib, "Analysis of the channel energy capture in ultra-wideband transmitted reference systems," *IEEE Trans. Commun.*, vol. 55, no. 2, pp. 262–265, Feb. 2007.

[35] M. Weisenhorn and W. Hirt, "Robust noncoherent receiver exploiting UWB channel properties," in *Proc. Internal Workshop on Ultra Wideband Systems Joint with Conf. Ultra Wideband Systems and Technologies, UWBST & IWUWBS*, Kyoto, Japan, May 2004, pp. 156–160.

[36] S. Zhao, P. Orlik, A. Molisch, H. Liu, and J. Zhang, "Hybrid ultrawideband modulations compatible for both coherent and transmit-reference receivers," *IEEE Trans. Wireless Commun.*, vol. 6, no. 7, pp. 2551–2559, July 2007.

[37] K. Witrisal, "A tutorial on noncoherent UWB systems," in Design and Analysis of Noncoherent UWB Transceivers, Sept. 2008, ch .1, Habilitation Thesis, Graz Univ. Technology. [Online]. Available: http://www.spsc.tugraz.at/people/klaus/WitrisalTutorial08.pdf

[38] L. Yang and G. Giannakis, "Optimal pilot waveform assisted modulation for ultrawideband communications," *IEEE Trans. Wireless Commun.*, vol. 3, no. 4, pp. 1236–1249, July 2004.

[39] N. Guo and R. Qiu, "Improved autocorrelation demodulation receivers based on multiple-symbol detection for UWB communications," *IEEE Trans. Wireless Commun.*, vol. 5, no. 8, pp. 2026–2031, Aug. 2006.

[40] A. D'Amico, U. Mengali, and E. Arias-de Reyna, "Energy-detection UWB receivers with multiple energy measurements," *IEEE Trans. Wireless Commun.*, vol. 6, no. 7, pp. 2652–2659, July 2007.

[41] G. Leus and A.-J. van der Veen, "A weighted autocorrelation receiver for transmitted reference ultra wideband communications," in *Proc. IEEE Signal Processing Workshop on Signal Processing Advances in Wireless Communications, SPAWC*, New York, NY, June 2005, 965–969.

[42] J. Romme and K. Witrisal, "Transmitted-reference UWB systems using weighted autocorrelation receivers," *IEEE Trans. Microwave Theory Tech.*, vol. 54, no. 4, pp. 1754–1761, Apr. 2006.

[43] Z. Tian and B. M. Sadler, "Weighted energy detection of ultra-wideband signals," in *Proc. IEEE Signal Processing Workshop on Signal Processing Advances in Wireless Communications, SPAWC*, New York, NY, June 2005, pp. 1068–1072.

[44] M. Weisenhorn and W. Hirt, "ML receiver for pulsed UWB signals and partial channel state information," in *Proc. IEEE Int. Conf. Ultra-Wideband, ICU*, Sept. 2005, pp. 180–185.

[45] Y.-L. Chao and R. Scholtz, "Ultra-wideband transmitted reference systems," *IEEE Trans. Veh. Technol.*, vol. 54, no. 5, pp. 1556–1569, Sept. 2005.

[46] T. Zasowski, F. Troesch, and A. Wittneben, "Partial channel state information and intersymbol interference in low complexity UWB PPM detection," in *Proc. IEEE Int. Conf. Ultra-Wideband, ICUWB*, Sept. 2006, pp. 369–374.

[47] C. Steiner and A. Wittneben, "Cognitive interference suppression for low complexity UWB transceivers," in *Proc. IEEE Int. Conf. Ultra-Wideband, ICUWB*, Hannover, Germany, Sept. 2008, pp. 165–168.

[48] C. Carbonelli and U. Mengali, "M-ppm noncoherent receivers for uwb applications," *IEEE Trans. Wireless Commun.*, vol. 5, no. 8, pp. 2285–2294, Aug. 2006.

[49] H. Luecken, T. Zasowski, C. Steiner, F. Troesch, and A. Wittneben, "Location-aware adaptation and precoding for low complexity IR-UWB receivers," in *Proc. IEEE Int. Conf. Ultra-Wideband, ICUWB*, Sept. 2008, pp. 31–34.

[50] K. Witrisal and M. Pausini, "Statistical analysis of UWB channel correlation functions," *IEEE Trans. Veh. Technol.*, vol. 57, no. 3, pp. 1359–1373, May 2008.

[51] M. Pausini and G. Janssen, "Performance analysis of UWB autocorrelation receivers over Nakagami-fading channels," *IEEE J. Select. Topics Signal Process.*, vol. 1, no. 3, pp. 443–455, Oct. 2007.

[52] K. Witrisal and M. Pausini, "Statistical analysis of transmitted-reference UWB systems on multipath channels," in *Proc. IEEE International Conf. Ultra-Wideband, ICUWB*, Waltham, MA, Sept. 2006, 303–308.

[53] H. Celebi and H. Arslan, "Cross-modulation interference and mitigation technique for ultrawideband PPM signaling," *IEEE Trans. Veh. Technol.*, vol. 57, no. 2, pp. 847–858, Mar. 2008.

[54] X. Dong, A. C. Lee, and L. Xiao, "A new UWB dual pulse transmission and detection technique," in *Proc. IEEE International Conf. Communications, ICC*, Seoul, Korea, May 2005, 2835–2839.

[55] D. I. Kim and T. Jia, "M-ary orthogonal coded/balanced ultra-wideband transmitted-reference systems in multipath," *IEEE Trans. Commun.*, vol. 56, no. 1, pp. 102–111, Jan. 2008.

[56] K. Witrisal, "Statistical analysis of the IEEE802.15.4a UWB PHY over multipath channels," in *Proc. IEEE Wireless Communications and Networking Conf., WCNC*, Las Vegas, NV, Apr. 2008, pp. 130–135.

[57] F. Troesch, F. Althaus, and A. Wittneben, "Pulse position pre-coding exploiting UWB power constraints," in *Proc. IEEE Signal Processing Workshop on Signal Processing Advances in Wireless Communications, SPAWC*, June 2005, pp. 395–399.

[58] F. Troesch, C. Steiner, T. Zasowski, T. Burger, and A. Wittneben, "Hardware aware optimization of an ultra low power UWB communication system," in *Proc. IEEE International Conf. Ultra-Wideband, ICUWB*, Sept. 2007, pp. 174–179.

[59] H. Lücken, T. Zasowski, and A. Wittneben, "Synchronization scheme for low duty cycle UWB impulse radio receiver," in *Proc. IEEE Int. Symp. Wireless Communication Systems, ISWCS*, Oct. 2008, pp. 503–507.

[60] C. Duan, P. Orlik, Z. Sahinoglu, and A. Molisch, "A non-coherent 802.15.4a UWB impulse radio," in *Proc. IEEE Int. Conf. Ultra-Wideband, ICUWB*, Sept. 2007, pp. 146–151.

[61] J. Ryckaert, G. Van der Plas, V. De Heyn, C. Desset, B. Van Poucke, and J. Craninckx, "A 0.65-to-1.4 nJ/burst 3-to-10 GHz UWB all-digital TX in 90 nm CMOS for IEEE 802.15.4a," *IEEE J. Solid-State Circuits*, vol. 42, no. 12, pp. 2860–2869, Dec. 2007.

[62] L. Yang and G. Giannakis, "Timing ultra-wideband signals with dirty templates," *IEEE Trans. Commun.*, vol. 53, no. 11, pp. 1952–1963, Nov. 2005.

[63] R. Djapic, G. Leus, A.-J. van der Veen, and A. Trindade, "Blind synchronization in asynchronous UWB networks based on the transmit-reference scheme," *EURASIP J. Wireless Commun. Netw.*, vol. 2006, no. 2, pp. 65–65, 2006.

[64] A. Schranzhofer, Y. Wang, and A.-J. van der Veen, "Acquisition for a transmitted reference UWB receiver," in *Proc. IEEE Int. Conf. Ultra-Wideband, ICUWB*, Hannover, Germany, Sept. 2008, pp. 149–152.

[65] L. Yang, G. B. Giannakis, and A. Swami, "Noncoherent ultra-wideband (de) modulation," *IEEE Trans. Commun.*, vol. 55, no. 4, pp. 810–819, Apr. 2007.

[66] A. D'Amico, U. Mengali, and L. Taponecco, "Energy-based TOA estimation," *IEEE Trans. Wireless Commun.*, vol. 7, no. 3, pp. 838–847, Mar. 2008.

[67] I. Guvenc and Z. Sahinoglu, "Threshold-based TOA estimation for impulse radio UWB systems," in *Proc. IEEE Int. Conf. Ultra-Wideband, ICU*, Sept. 2005, pp. 420–425.

[68] I. Guvenc, Z. Sahinoglu, and P. Orlik, "TOA estimation for IR-UWB systems with different transceiver types," *IEEE Trans. Microwave Theory Tech.*, vol. 54, no. 4, pp. 1876–1886, June 2006.

[69] Y.-S. Kwok, F. Chin, and X. Peng, "Ranging mechanism, preamble generation, and performance with IEEE 802.15.4a low-rate low-power UWB systems," in *Proc. IEEE Int. Conf. Ultra-Wideband, ICUWB*, Sept. 2006, pp. 525–530.

[70] M. Pausini and G. J. M. Janssen, "On the narrowband interference in transmitted reference UWB receivers," in *Proc. IEEE Int. Conf. Ultra-Wideband, ICU*, Zurich, Switzerland, Sept. 2005, pp. 571–575.

[71] T. Quek, M. Win, and D. Dardari, "Unified analysis of UWB transmitted-reference schemes in the presence of narrowband interference," *IEEE Trans. Wireless Commun.*, vol. 6, no. 6, pp. 2126–2139, June 2007.

[72] Y. D. Alemseged and K. Witrisal, "Modeling and mitigation of narrowband interference for transmitted-reference UWB systems," *IEEE J. Select. Topics Signal Process.*, vol. 1, no. 3, Oct. 2007, pp. 456–469.

[73] C. Steiner and A. Wittneben, "On the interference robustness of ultra-wideband energy detection receivers," in *Proc. IEEE Int. Conf. Ultra-Wideband, ICUWB*, Singapore, Sept. 2007, pp. 721–726.

[74] A. Rabbachin, T. Quek, P. Pinto, I. Oppermann, and M. Win, "UWB energy detection in the presence of multiple narrowband interferers," in *Proc. IEEE Int. Conf. Ultra-Wideband, ICUWB*, Singapore, Sept. 2007, pp. 857–862.

[75] Q. H. Dang and A.-J. van der Veen, "Narrowband interference mitigation for a transmitted reference ultra-wideband receiver," in *Proc. European Signal Processing Conf., EUSIPCO*, Florence, Italy, Sept. 2006.

[76] K. Witrisal, "Noncoherent autocorrelation detection of orthogonal multicarrier UWB signals," in *Proc. IEEE Int. Conf. Ultra-Wideband, ICUWB*, Hannover, Germany, Sept. 2008, pp. 161–164.

[77] L. Feng and W. Namgoong, "An oversampled channelized UWB receiver with transmitted reference modulation," *IEEE Trans. Wireless Commun.*, vol. 5, no. 6, pp. 1497–1505, June 2006.

[78] S. Lee, S. Bagga, and W. Serdijn, "A quadrature downconversion autocorrelation receiver architecture for UWB," in *Proc. Internal Workshop on Ultra Wideband Systems Joint with Conf. Ultra Wideband Systems and Technologies, UWBST & IWUWBS*, May 2004, pp. 6–10.

[79] M. Pausini and G. J. M. Janssen, "Narrowband interference suppression in transmitted reference UWB receivers using sub-band notch filters," in *Proc. European Signal Processing Conf., EUSIPCO*, Florence, Italy, Sept. 2006.

[80] F. Dowla, F. Nekoogar, and A. Spiridon, "Interference mitigation in transmitted-reference ultra-wideband (UWB) receivers," in *Proc. IEEE Antennas and Propagation Society Int. Symp. 2004.*, June 2004, vol. 2, pp. 1307–1310.

[81] C. Krall, K. Witrisal, G. Leus, and H. Koeppl, "Minimum mean squared error equalization for second-order Volterra systems," *IEEE Trans. Signal Process.*, vol. 56, no. 10, pp. 4729–4737, Oct. 2008.

[82] V. Lottici and Z. Tian, "Multiple symbol differential detection for UWB communications," *IEEE Trans. Wireless Commun.*, vol. 7, no. 5, pp. 1656–1666, May 2008.

[83] M. Sahin and H. Arslan, "Inter-symbol interference in high data rate UWB communications using energy detector receivers," in *Proc. IEEE Int. Conf. Ultra-Wideband, ICU*, Sept. 2005, pp. 176–179.

[84] S. Paquelet, L.-M. Aubert, and B. Uguen, "An impulse radio asynchronous transceiver for high data rates," in *Proc. Internal Workshop on Ultra Wideband Systems Joint with Conf. Ultra Wideband Systems and Technologies, UWBST & IWUWBS*, Kyoto, Japan, May 2004, pp. 1–5.

[85] M. Mroue, S. Haese, S. Paquelet, S. Mallegol, and G. El-Zein, "An implementation study of an analog CMOS detector for IR-UWB non-coherent receiver," in *Proc. IEEE Int. Workshop on Radio-Frequency Integration Technology, RFIT*, Dec. 2007, pp. 13–16.

[86] M. Penaloza, G. Baudoin, M. Villegas, and L. Montes, "BAW filter bank for an UWB multi band on-off keying transceiver," in *Proc. Microwave Conf., 2007. APMC 2007. Asia-Pacific*, Dec. 2007, pp. 1–4.

[87] J. Romme, "UWB channel fading statistics and transmitted reference communication," Ph.D. dissertation, Graz Univ. Technology, Austria, Mar. 2008.

[88] E. Fishler and H. Poor, "On the tradeoff between two types of processing gains," *IEEE Trans. Commun.*, vol. 53, no. 10, pp. 1744–1753, Oct. 2005.

[89] T. Jia and D. I. Kim, "Multiple access performance of balanced UWB transmitted-reference systems in multipath," *IEEE Trans. Wireless Commun.*, vol. 7, no. 3, pp. 1084–1094, Mar. 2008.

[90] C. Steiner and K. Witrisal, "Multiuser interference modeling and suppression for a multichannel differential IR-UWB system," in *IEEE Int. Conf. Ultra-Wideband*, ICU, Zurich, Switzerland, Sept. 2005, pp. 667–672.

[91] Z. Xu and B. M. Sadler, "Multiuser transmitted reference untra-wideband communication systems," *IEEE J. Select. Areas Commun.*, vol. 24, no. 4, pp. 766–772, Apr. 2006.

[92] A. F. Molisch, *Wireless Communications*. Hoboken, NJ: Wiley, 2005.

[93] S. Song and Q. Zhang, "TH-CDMA-PPM with noncoherent detection for low rate WPAN," *IEEE Trans. Wireless Commun.*, vol. 7, no. 2, pp. 446–451, Feb. 2008. [SP]